

AD-A043 280

SCIENCE APPLICATIONS INC MCLEAN VA
A HEAT TRANSFER STUDY IN FOLDED AMMUNITION GUN TUBE CHAMBERS. (U)

F/G 19/6

UNCLASSIFIED

JUL 77 P L VERSTEEGEN, F D VARCOLIK

DAAD05-76-C-0782

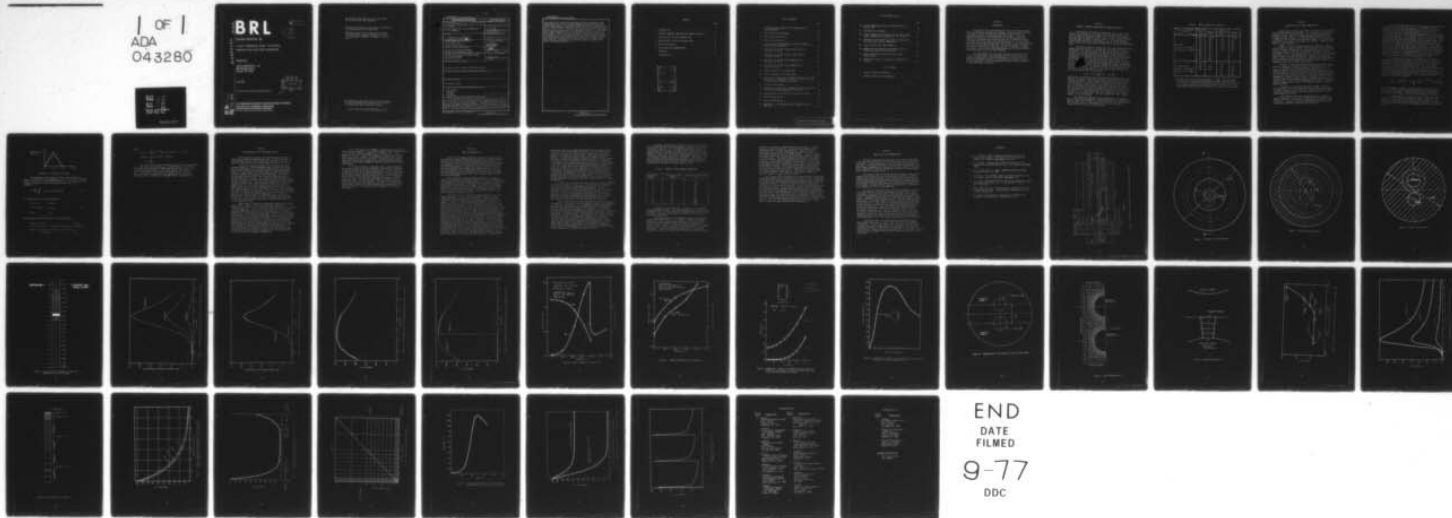
SAI-76-653-WA

BRL-CR-342

NL

1 OF 1
ADA
043280

BRL



END
DATE
FILMED
9-77
DDC

BRL CR 342

BRL

AD

12
NW

AD A 043280

CONTRACT REPORT NO. 342

A HEAT TRANSFER STUDY IN FOLDED
AMMUNITION GUN TUBE CHAMBERS

Prepared by

Science Applications, Inc.
8400 Westpark Drive
McLean, VA 22101

July 1977

DDC
RECEIVED
AUG 22 1977
RECEIVED

Approved for public release; distribution unlimited.

gr

B

AD No. _____
DDC FILE COPY

USA ARMAMENT RESEARCH AND DEVELOPMENT COMMAND
USA BALLISTIC RESEARCH LABORATORY
ABERDEEN PROVING GROUND, MARYLAND

Destroy this report when it is no longer needed.
Do not return it to the originator.

Secondary distribution of this report by originating
or sponsoring activity is prohibited.

Additional copies of this report may be obtained
from the National Technical Information Service,
U.S. Department of Commerce, Springfield, Virginia
22151.

The findings in this report are not to be construed as
an official Department of the Army position, unless
so designated by other authorized documents.

*The use of trade names or manufacturers' names in this report
does not constitute indorsement of any commercial product.*

UNCLASSIFIED

SECURITY CLASSIFICATION OF THIS PAGE (When Data Entered)

18 BRL 19 CR-342

REPORT DOCUMENTATION PAGE		READ INSTRUCTIONS BEFORE COMPLETING FORM
1. REPORT NUMBER BRL CONTRACT REPORT NO. 342 ✓	2. JOVLT ACCESSION NO.	3. RECIPIENT'S CATALOG NUMBER
4. TITLE (and Subtitle) A HEAT TRANSFER STUDY IN FOLDED AMMUNITION GUN TUBE CHAMBERS	5. TYPE OF REPORT & PERIOD COVERED Final Report ✓	6. PERFORMING ORG. REPORT NUMBER SAI-76-653-WA
7. AUTHOR(s) P. L. Versteegen, F. D. Varcolik, N. E. Banks, G. J. Klem	8. CONTRACT OR GRANT NUMBER(s) DAAD05-76-C-0782 new	10. PROGRAM ELEMENT, PROJECT, TASK AREA & WORK UNIT NUMBERS 1F266201DH96 LR & D-843-76
9. PERFORMING ORGANIZATION NAME AND ADDRESS Science Applications, Inc. 8400 Westpark Drive McLean, Virginia 22101	11. CONTROLLING OFFICE NAME AND ADDRESS USA Ballistics Research Laboratory Aberdeen Proving Ground, MD 21005	12. REPORT DATE JUL 1977
14. MONITORING AGENCY NAME & ADDRESS (if different from Controlling Office) USA Material Development & Readiness Command 5001 Eisenhower Avenue Alexandria, VA 22333	13. NUMBER OF PAGES 42	15. SECURITY CLASS. (of this report) UNCLASSIFIED
15a. DECLASSIFICATION/DOWNGRADING SCHEDULE		
16. DISTRIBUTION STATEMENT (of this Report) Approved for public release; distribution unlimited		
17. DISTRIBUTION STATEMENT (of the abstract entered in Block 20, if different from Report)		
18. SUPPLEMENTARY NOTES COR: Norman E. Banks		
19. KEY WORDS (Continue on reverse side if necessary and identify by block number) HEAT TRANSFER CONDUCTION GUN TUBES TEMPERATURE		
20. ABSTRACT (Continue on reverse side if necessary and identify by block number) → Time dependent heat transfer analyses have been performed for folded gun tube chambers in that part of the gun tube that is sandwiched between the folded part of the shell casing and the projectile. The asymmetric configuration was believed to introduce 3-dimensional effects so that peak temperatures could not be determined adequately by 2-dimensional analyses. Calculations performed, however, showed that for the single round firing of a projectile a 1-dimensional representation could adequately estimate the peak temperature except for the interior →		

408 404

UNCLASSIFIED

SECURITY CLASSIFICATION OF THIS PAGE(When Data Entered)

corner region of the propellant capsule which required a 2-dimensional model. A representative set of time- and space-dependent gas temperatures and heat transfer coefficients for conventional unfolded ammunition was supplied by BRL. Maximum surface temperatures were found to occur at a region (named Location 13) near the origin of rifling. Data from this location was used for a 1-dimensional analysis of a non-corner region and a 2-dimensional analysis of a corner region. The calculated temperature rise for an SAE 4340 steel non-corner surface was 1003°C (1836°F). When a brass layer was used to simulate the cartridge case, the temperature rise was only 660°C (1220°F) for a non-corner region. However, for a corner region, the brass-coated surface temperature reached a maximum of 1099°C (2010°F). The results for the interior corner are only tentative because significant approximations were required to model the geometry and to specify the boundary conditions.

UNCLASSIFIED

SECURITY CLASSIFICATION OF THIS PAGE(When Data Entered)

CONTENTS

	Page
1. INTRODUCTION	1
2. GEOMETRY, BOUNDARY CONDITIONS AND THERMAL PROPERTIES	2
3. DESCRIPTION OF THE HEAT TRANSFER CODE	3
4. MODIFICATIONS TO THE HEAT TRANSFER CODE	8
5. ANALYSIS AND RESULTS	10
6. CONCLUSIONS AND RECOMMENDATIONS	14
REFERENCES	15
DISTRIBUTION LIST	41

ACCESSION for		
NTIS	White Section	<input checked="" type="checkbox"/>
DDC	Buff Section	<input type="checkbox"/>
UNANNOUNCED		<input type="checkbox"/>
JUSTIFICATION		
BY		
DISTRIBUTION/AVAILABILITY CODES		
Dist.	AVAIL	or SPECIAL
A		

LIST OF FIGURES

	Page
1. Longitudinal Cross Section of a Folded Ammunition Gun Tube Chamber	16
2. End View of the Breech Region	17
3. View of Cross Section B-B	18
4. View of Cross Section C-C	19
5. Cross Section of the Geometry for Which the Boundary Conditions were Generated	20
6. Time Histories of Heat Transfer Coefficients at Locations 1, 6 and 12	21
7. Time Histories of Heat Transfer Coefficients at Locations 13 and 15	22
8. Time Histories of Bulk Fluid Temperatures at Locations 1, 6 and 12	23
9. Time Histories of Bulk Fluid Temperatures at Locations 13 and 15	24
10. Thermal Properties of SAE 4340 Steel	25
11. Thermal Properties of Cartridge Brass	26
12. Comparison of Theoretical and TRUMP Calculated Temperature Profiles for a Rectangular Slab with a Constant Heat Flux on One Face and Insulated on the Other	27
13. Triangular Pulse Shape	6
14. Comparison of Theoretical and TRUMP Calculated Temperature Profiles for a Spike Shaped Heat Flux Profile.	28
15. Representative Cross Section of the Gun Tube Chamber . . .	29
16. Node Configuration No. 3	30
17. Node Configuration No. 5	31
18. Dependency of the Computed Surface Temperature on the Node Size	32

LIST OF FIGURES (Cont.)

	Page
19. Surface Temperature History at Three Locations on the Gun Tube	33
20. Configuration 11 Geometry	34
21. Spatial Temperature Distribution at the Time of Peak Surface Temperature at Locations 13, 15, 16 and 17	35
22. Temperature Distribution Across Web at Location 13 at the Time of Peak Surface Temperature	36
23. Interior Corner Region Node Geometry	37
24. Temperature-Time History for the Interior Corner Region Peak Temperature Surface Node	38
25. Spatial Temperature Profiles for the Interior Corner Region	39
26. Temperature History of Location 12 for Multiple (3) Firings.	40

LIST OF TABLES

1. Thermal Properties of Materials	3
2. Summary of Peak Surface Temperatures	12

Section 1

INTRODUCTION

The analysis and results described in this report were performed under a contract with the Ballistics Research Laboratories (BRL) entitled "Transient 3-D Finite-Difference Calculations of Heat Transfer and Temperature Profiles in 30-mm Folded Gun Tube Chambers." The major emphasis was placed on the determination of the time-dependent heat transfer in the chamber part of the gun tube that is sandwiched between the folded part of the shell casing and the projectile. It was anticipated that 3-dimensional effects would be important in obtaining reasonably accurate results of peak temperatures. BRL was developing a 3-D Monte Carlo code to evaluate such cases, but had not yet completely debugged the program. Since results were needed quickly the 3-D finite difference methods available at SAI were deemed adequate.

The peak temperatures were to be evaluated for the case of the firing of a single round. As a shakedown test of the method, BRL has supplied representative information developed from interior ballistics codes for an unfolded 37-mm gun. These boundary conditions were time- and space-dependent local gas temperatures and heat transfer coefficients at the gas-gun metal interface.

Section 2

GEOMETRY, BOUNDARY CONDITIONS AND THERMAL PROPERTIES

The available description of the geometry was in the form of sketches and drawings of a prototype folded gun tube assembly. From these, a composite drawing and several cross sections were prepared that described the geometry in terms useful for heat transfer analyses. These drawings are shown in Figures 1 thru 4. They show the basic dimensions and materials of the assembly. Except for the cartridge, which is made of cartridge brass, the material is assumed to be SAE 4340 steel.

The primary region of interest was in the web between the powder chamber and the projectile in the area near the origin of rifling, approximately 4.5 inches from the rear face of the breech ring shown in Figure 1. The peak temperatures experienced by the gun barrel assembly were to be determined in that region for the single firing of a projectile. The boundary conditions interior to the gun barrel were provided by BRL in the form of heat transfer coefficients and bulk fluid temperatures as a function of time and position along the gun barrel. The boundary conditions consisted of approximately 1300 cards in a form readily usable for analysis by computer. They contained data describing the variation of the heat transfer coefficient, h , and bulk fluid temperatures, T_b , as a function of time, t , and location along the interior of the gun barrel, z . The heat flow per unit area, q'' , into the gun barrel was then defined as:

$$q''(z,t) = h(z,t) \left[T_b(z,t) - T_s(z,t) \right]$$

where $T_s(z,t)$ is the barrel surface temperature to be determined. The data for the boundary conditions are actually applicable to a straight projectile geometry. Figure 5 shows the locations for which data are provided and the relative location of the projectile at early times. Since the boundary condition set is too large to be presented here, only a few figures are supplied to show typical behavior and magnitude. The early time heat transfer coefficients for locations 1, 6 and 12 are displayed in Figure 6 while those for locations 13 and 15 are shown in Figure 7. The corresponding bulk fluid temperatures are shown in Figures 8 and 9, respectively. The data are given for every 0.00005 seconds out to 0.02 seconds.

The temperature-dependent thermal properties of the materials used in the gun tube assembly are taken from Reference 2. Values for specific heat, thermal conductivity, and density for both SAE 4340 steel and cartridge brass are shown schematically in Figures 10 and 11, respectively, and are also listed in Table 1.

Table 1. Thermal Properties of Materials

Material \ Properties	Specific Heat (J/kg-C)	Temperature (C)	Thermal Conductivity (W/m-C)	Temperature (C)
SAE 4340 Density: 7,750 kg/m ³ Melting Point: 1450°C	502.	-18.05	43.1	-18.05
	519.	204.	42.3	204.
	619.	427.	38.6	427.
	753.	648.	32.2	648.
	800.	763.	25.9	788.
	6895.*	768.	27.0	871.
	628.	773.		
	586.	871.		
	607.	1094.		
Cartridge Brass Density: 8,570 kg/m ³ Melting Point: 940°C	398.	0.	96.	0.
	490.	200.	105.	100.
	527.	500.	109.	200.
			113.	300.
			115.	400.

* SAE 4340 steel has a solid phase change at $\sim 768^{\circ}\text{C}$. The latent heat involved in this transition is modeled by a change in specific heat in the form of a spike superimposed over the actual specific heat curve. This triangular peak has a base width of 10°C , a height of $1/5$ of the latent heat of transition and is centered at the transition temperature.

Section 3

DESCRIPTION OF THE HEAT TRANSFER CODE

The various calculations described in this report were performed with the TRUMP computer program (Ref. 1). This program was developed originally at LRL, Livermore primarily for research and development related to nuclear energy. The TRUMP code was obtained by SAI from A. Edwards of LRL, Livermore in early 1975 and modified to run with the standard CDC Fortran compiler and operating systems. It has been used successfully on a number of heat conduction problems. Capabilities of TRUMP are summarized below.

TRUMP is a digital computer program for transient or steady state analyses of flows in various kinds of potential fields in complex systems. Examples include heat flow in temperature fields, mass flow in pressure fields, and current in electrical and magnetic fields; they often include various sources and sinks, and modes of transport other than potential flow. The program allows solution of a general nonlinear parabolic partial differential equation. Two additional equations, which in thermal problems represent heat production by decomposition of reactants having rate constants with a general Arrhenius temperature dependence, may also be solved simultaneously.

Solutions to both steady-state and transient problems may be obtained. Geometric configurations may be quite complex, with flow in 1-, 2-, or 3-dimensions; with rectangular, cylindrical, axial, or spherical symmetry; or with arbitrary shape and structure. Initial conditions may vary with spatial position. Material properties, source and sink strengths, boundary conditions, and other problem parameters may vary with spatial position, time, or the primary dependent variable (temperature, pressure, field strength). External sources or sinks, coupled to the system by means of specified boundary conditions, may vary with time. Certain problem parameters at one spatial location may be made to depend on the value of the dependent variable at another spatial location.

Limitations of the program include the number of spatial locations which can be calculated (which may be from several hundred to several thousand in various versions) and the amount of computer time required (which may be from a few seconds up to hours for the largest possible problems).

Input data are efficiently organized to be as simple and compact as possible. Output data include numerical, graphical, and punched card data, with options on frequency and content controlled by the user. Output is organized and labeled to provide the user with maximum information concerning the calculation.

Part of the TRUMP Program is a file containing thermal properties of a great variety of materials (Ref. 2). The TRUMP Program can process this file to retrieve appropriate data for those materials requested by the problem input description. The data on this file include densities, transition temperatures, heats of transition, and tables of specific heat and thermal conductivity versus temperature, for over 1000 materials. An alphabetical material index, list of data sources, material-classification system, data-quality indicator system, and the data themselves are on computer cards and magnetic tapes. The data are in the format used for material property input data in the TRUMP Program. Processing options available with the TRUMP Program include: (a) reading the material data, checking for various types of format errors, calculating table slopes, calculating enthalpies from specific heat tables, and writing out the input data, error diagnostics, and calculated data; (b) converting material data to any desired unit system; (c) producing a secondary material data list from the master data list, including all the materials or only the materials on a material selection list; and (d) any combinations of these.

The adequacy and accuracy of the TRUMP code for calculating temperature distributions has been verified by comparing results obtained with TRUMP against analytical solutions of the same problems. Two problems reflecting characteristics similar to those found in gun tube heat transfer problems were chosen. The first problem consists of a slab of steel 10 cm thick with one side insulated and the other exposed to a constant heat flux. The geometry and critical conditions are shown in Figure 12 together with selected results. The theoretical temperature distribution at any time and any position is taken from Carslaw and Jaeger (Ref. 3) and is given by Equation 1. The results, as predicted by Equation 1

$$T = \frac{\phi t}{\rho C_p \ell} + \frac{\phi \ell}{k} \left\{ \frac{3x^2 - \ell^2}{6\ell^2} - \frac{2}{\pi^2} \sum_{n=1}^{\infty} \frac{(-1)^n}{n^2} e^{-\alpha t \left(\frac{n\pi}{\ell}\right)^2} \cos\left(\frac{n\pi x}{\ell}\right) \right\} \quad (1)$$

and as calculated by TRUMP, are shown in Figure 12 for two different times. The TRUMP calculations were performed with a 20-node mesh description. The thermal properties used for the calculations are also given in the figure. As may be noted agreement is excellent.

The second problem is very similar to conditions existing in the gun tube. A semi-infinite solid made of steel is subjected at the surface to a spike heat flux of the form shown in Figure 13. The duration of the spike and its magnitude are of the order of those that might be found with the geometry and boundary conditions discussed in Section 2.

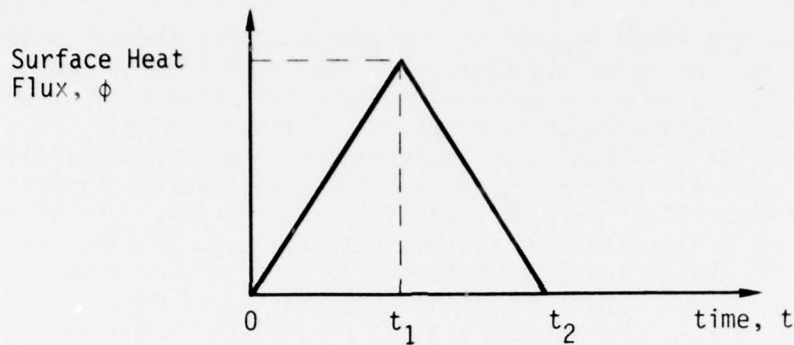


Figure 13. Triangular Pulse Shape

The temperature distribution in a semi-infinite solid in a region $x > 0$ initially at zero temperature, for a flux $\phi(t)$ per unit area per unit time at $x = 0$, with heat ceasing at $x = 0$ at time t_2 , and then thermally insulated is given by Carslaw and Jaeger (Ref. 3) as Equation 2.

$$T = \frac{\sqrt{k/\pi}}{K} \int_0^t \phi(t-\tau) \exp(-x^2/4k\tau) \frac{d\tau}{\sqrt{\tau}}. \quad (2)$$

For a heat flux, $\phi(t)$, given by Equation 3,

$$\begin{aligned} \phi(t) &= at & 0 < t \leq t_1 \\ \phi(t) &= b(t-t_1) & t_1 < t \leq t_2 \\ \phi(t) &= 0 & t > t_2 \end{aligned} \quad (3)$$

the solution to the above problem is given by Equation 4

$$\begin{aligned} T(x,t) &= a V(x,t) & 0 < t \leq t_1 \\ T(x,t) &= a V(x,t) - a V(x,t-t_1) + b V(x,t-t_1) & t_1 < t \leq t_2 \\ T(x,t) &= a V(x,t) - a V(x,t-t_1) + b V(x,t-t_1) - b V(x,t-t_2) & t > t_2 \end{aligned} \quad (4)$$

where

$$V(x,t) = \frac{2\sqrt{k}}{3K} (t)^{3/2} \left[2(1+Y^2) \text{ierfc}(Y) - Y \text{erfc}(Y) \right]$$

$$\text{ierfc}(Y) = \frac{1}{\sqrt{\pi}} \exp(-Y^2) - Y \text{erfc}(Y)$$

$$Y^2 = \frac{x^2}{4k\tau}$$

The analytical solution is plotted in Figure 14 for the condition $t_1 = 1$ msec, $t_2 = 6.5$ msec, and $\phi_{\max} = 3.32 \times 10^8$ Watt/m². The TRUMP calculations were performed with the same geometry description as used in the gun tube calculations. This configuration, identified as No. 11 is described in more detail in the next section. As may be noted from Figure 14 where the surface temperature is plotted as a function of time, the analytical and TRUMP results agree quite well.

Section 4

MODIFICATIONS TO THE HEAT TRANSFER CODE

Various computer programs and subroutines were developed in order to facilitate data handling processes. Since the computations with TRUMP were done on the CDC 7600 at the ARC, Huntsville, AL, several of the programs were oriented toward the use of that system.

The primary modifications dealt with the processing of the boundary conditions. The time-dependent heat transfer coefficients and fluid bulk temperatures are used by TRUMP in the form of tables. At any time during the calculational process the code interpolates linearly in these tables to get the current or projected values of the heat transfer coefficient and fluid temperature. The version of the code operational at the ARC is set up to accept tables with a maximum length of 12 entries. This is far less than the number of data points actually available, which numbers approximately 300 values. In order to handle such a large data set a program was written to read the data provided by BRL, convert the heat transfer coefficients and temperatures to a set of units compatible with the other data for TRUMP, compute the derivatives of these values with respect to time, and store the results on a file that TRUMP can access. Three routines were added to TRUMP to process and use this file. One routine retrieves from the file the data set appropriate to the axial location along the gun barrel of interest and stores these data in the Large Core Memory (LCM) of the CDC 7600. The other two routines retrieve data in groups of 12 sets from LCM for the time interval under computation. As time increases appropriate data sets are processed and stored in the available table space.

TRUMP computes its own time step based on stability and several error criteria. Because the time span over which the maximum temperature is reached is small, the time step in TRUMP has to be limited to the maximum value. If such a restriction were not imposed the time step that TRUMP would compute prior to the sudden rise in the heat transfer coefficient would be so large that interpolation of the tables would result in values that passed the peak. The limitation on the time step resulted in a great deal of output which, instead of being printed, could be stored and catalogued as a permanent file. Two programs were written to process this results file. The first one retrieved and printed data for selected nodes and time intervals, while the second one produced printer plots of the temperature-time histories of selected nodes and spatial temperature distributions at selected times. The first program was used for normal test runs and served basically to isolate time spans and regions of interest. The second one was used to produce more detailed results for evaluation. The second program also has the ability to generate CALCOMP plots.

Part of the input data to TRUMP is a detailed description of all nodes and node connections. For problems with many nodes the determination of all node and connection parameters is a laborious task. For geometries that can be described by bodies of revolution, the FED(4) program can be used. However, for rectangular 2-dimensional problems this program was found to be unsuitable. A separate program, named TODXY, was hence written to generate the node and connection data for rectangular 2-dimensional geometries such as the one near the interior corner region.

As will be discussed in more detail later, it was found that the use of a single firing did not produce large temperature changes at large distances from the bore inside surface. To get a feel for how multiple firing affects the temperature distributions a subroutine was written to recycle the boundary conditions. It was assumed that the available boundary conditions would also be valid for the second round of firing so that the only requirement was to add a constant to the time base. A routine was incorporated in TRUMP to test the progress of time in the calculations. If it were to exceed the last entry of the 12 value table, the times specified in this table would be modified by adding to each entry the difference between the last and first entries. A test case with this capability is discussed in Section 5.

Section 5

ANALYSIS AND RESULTS

Based on the boundary conditions supplied it was obvious that the most active region extended from the base of the folded ammunition cartridge to a distance just beyond the nose of the projectile. A cross-sectional view of the gun tube taken anywhere within this region was assumed to be the same so that for initial purposes the problem could be represented by a 2-dimensional model of a series of slices, which when stacked on one another, would define the entire region. Figure 15 shows the basic 2-dimensional cross-section as it was used. This cross-section was then divided into a series of nodes for which the time-dependent temperatures were to be computed using the finite difference code TRUMP.

The code requires that each node be defined by a volume, a material type, and heat flow paths to other nodes in the configuration. The accuracy of the calculated temperatures is, in general, conditioned by the fineness of the mesh. The finer the mesh the more accurate predictions of temperatures one can make. This does not come without some sacrifices; in this case, increased computer execution time and insufficient central memory locations. The procedure used here to develop a proper model was an effort to minimize the number of nodes while maintaining reasonable accuracy.

The first series of calculations used constant values for the thermal properties, specific heat and thermal conductivity, and an approximate history of the boundary conditions. The heat transfer coefficients and bulk temperatures were approximated by several line segments. Three of the models analyzed are shown in Figures 16, 17, and 20. The first of these, which is labeled as Configuration 3, was the product of two attempts to subdivide the entire cross-section into nodes. Results indicated that these were poor nodal mesh designs, since not much was observed to happen in terms of short-term temperature rises. The calculations revealed that only nodes very near the chamber walls (nodes 1 thru 48 and 101-148) were experiencing any temperature change. These temperatures were also found to be independent of the circumferential location at equal distances from the chamber walls. For these reasons the nodal structure was further simplified by analyzing only a small region near the chamber wall as shown in Figure 17. This configuration produced the exact same results as the one shown in Figure 16. Various configurations were then devised to study the effect of the mesh size on calculated temperatures. Each successive configuration was obtained by approximately halving the size of the node of the previous geometry. Surface temperatures were computed using the approximate boundary conditions of location 6 (see Figure 5) and constant thermal properties. The results are shown in Figure 18. The dependency of the surface temperature on the node size is readily seen in this figure. With the last

configuration the surface temperature histories at several locations along the gun-barrel are shown in Figure 19. The last configuration tested, No. 10, showed that the region of significant temperature changes in the metal was confined within a very narrow distance from the wall. A temperature change of less than 1 degree at the time the surface temperature reached a maximum value was experienced beyond a distance of 0.085 cm and (0.033 inch) from the wall. Furthermore, in the region of the highest heat transfer coefficient, axial variation of the coefficients themselves and their associated bulk temperatures is not very significant as may be observed from Figures 6 thru 9. Hence, for a single firing case, when the initial material temperature is everywhere the same, the peak temperature is not expected to be influenced by the neighboring conditions. It was thus decided that a 1-dimensional representation of a single firing case would provide adequate estimates of peak surface temperatures. A final configuration was then developed to provide the accuracy near the surface and a smoothly developing profile into the solid. Configuration 11 is shown in Figure 20.

To verify the assumption that axial conduction could be neglected in the case of a single firing, an r-z calculation was performed with five (5) axial meshpoints corresponding to Locations 13 thru 17 for which heat transfer coefficient data were specified. The mesh configuration in the r-direction was the same as the one for Configuration 11 except that only the first 20 nodes near the bore surface were used. The resulting temperature distributions, using this 2-D model, were found to be identical to those generated by 1-D analyses, confirming the 1-dimensional nature of the present problem. All remaining calculations were then performed with Configuration 11.

Table 2 shows results of nine calculations performed with this configuration. Calculation 1 used the simplified set of input parameters as in previous calculations; i.e., constant heat capacity and thermal conductivity, and the heat transfer coefficient and bulk temperature histories approximated by 11 straight line segments. Calculation 2 was made with temperature-dependent heat capacity and thermal conductivity. Calculation 3 used the full set of heat transfer coefficients and bulk temperatures as supplied by BRL. Calculations 4 thru 8 were similar to Calculation 3 except that the boundary conditions for Locations 12 and 14 thru 17 were used. Calculation 9 is similar to 3 except that Cartridge Brass was the material into which the heat flow occurred. As may be noted from Table 2 the peak surface temperature is approximately 1000°C (1830°F). The effect of brass compared to steel is to reduce the peak temperature by about 34%. The spatial temperature distributions for Calculations 3, 6, 7, and 8 at the time that the peak surface temperature is reached are shown in Figure 21.

The spatial temperature distribution across the whole web at the time when the peak surface temperature is reached at Location 13 is shown in Figure 22. This configuration consisted of two No. 11 configurations back-to-back. The heat transfer coefficient in the powder region was approximated by folding the 1-D boundary condition geometry, Figure 5, into the folded chamber geometry, Figure 1, and choosing the equivalent location for the boundary conditions; in this case Location 12 would be opposite to Location 13. The effects of brass on these calculations were not included. These calculations basically show that the opposite wall has no effect on the peak temperature in the case of a single round of firing.

Table 2. SUMMARY OF PEAK SURFACE TEMPERATURES

Calculation Number	Gun Tube Location Number	Peak Surface Temperature (°C)
1	13	939.
2	13	984.
3	13	1003.
4	12	932.
5	14	973.
6	15	979.
7	16	968.
8	17	950.
9	13	660.

In addition to Calculation No. 9 of Table 2 a 1-dimensional analysis was performed for a case when the proper brass thickness was followed by steel. Perfect contact was assumed between the brass and the steel. The results were identical to those of Calculation No. 9 for the peak temperature.

A large temperature rise is expected to occur in the interior corner region identified by "4" in Figure 1. Appropriate boundary conditions for this region were not available. They are expected to deviate from the conventional ammunition boundary conditions of Figure 5, and are certain to be a function of the radius of curvature of this region. To get an estimate of the magnitude of the effect of the corner a 2-dimensional model was constructed. The corner was assumed to be square, no rounded edge in other words, with the boundary

conditions for Location 13 applied over the whole region. The node geometry is shown in Figure 23. The material was assumed to be Cartridge Brass for the whole configuration. Figure 24 shows the temperature history of the surface node closest to the corner. The peak temperature reached here is 1099°C (2010°F). Figure 25 shows two temperature profiles at the time the surface temperature has reached its maximum value. The upper curve shows how the surface temperature varies as a function of distance away from the corner. As noted an asymptotic value of 668°C is reached at approximately 0.10 cm. This corresponds to the 1-D calculation, No. 9 of Table 2. The difference between 668°C and 660°C is due to the coarser nodal structure used in the 2-D model. The lower curve shows the temperature distribution along the diagonal shown in Figure 23. Here again the maximum region of influence extends to about 0.10 cm. These results appear to imply that rounding edges to 1/32" radius can substantially reduce 2-D effects in case of a single round of firing.

As discussed above, the material thickness over which significant temperature changes occur is very thin for a single firing. To determine the feasibility of performing multiple firings and to analyze its effects on the temperature distribution the boundary conditions were modified as discussed in Section 4. Results of a case with three firings using configuration 10 are shown in Figure 26. A firing frequency of 600 rounds per minute was assumed. As may be noted, the peak surface temperatures increase several tens of degrees from round-to-round which is expected. The material layer experiencing significant temperature changes increases with each round. With configuration 10, after the third round, the last node farthest away from the surface is at a temperature of 54°C. This shows that 3-dimensional effects are becoming important. The temperature rise from round-to-round does not result entirely from the multiple firing condition, but also from inadequate modeling for this case. Further study is required to determine more exact temperatures.

Section 6

CONCLUSIONS AND RECOMMENDATIONS

The results presented and discussed in this report showed that, in the case of a single firing, 1-D and 2-D analyses were sufficient to describe peak surface temperatures in non-corner and corner regions respectively. A 3-dimensional analysis did not result in any better estimates of peak temperatures for the case of a single round of firing, but may be important for long-term temperature variations in the web region and for cases of multiple firings.

The interior corner of the web region was shown to reach a peak temperature 70% higher than the non-corner region (1099°C vs. 660°C). However, since the spatial detail of the heat transfer coefficients was insufficient and the available boundary conditions were inappropriate for the folded ammunition geometry, significant approximations were made which prevent an accurate determination of the peak surface temperature of the corner. Further work must be done to obtain more suitable boundary conditions for input to the TRUMP code.

For the case of multiple firings the folded geometry may have a significant effect on the peak temperature of the web region. Such a case requires a more detailed analysis than presented in this report. A number of improvements are possible with the presently available techniques. Temperature distributions can be generated with boundary conditions specific to the folded ammunition case. This may require a slight modification to the TODXY program in order to handle the more detailed spatial resolution. With a good set of boundary conditions the multiple firing case can be evaluated in more detail and 3-dimensional effects can be included properly. Such cases require considerable computer time and memory. Areas within TRUMP have already been identified where significant improvements with respect to these two items can be made. The effects of web thickness, cartridge thickness, contact resistance between brass and steel, bore surface coatings, radiation between the propellant gases and the chamber surfaces, friction of the projectile with the gun barrel can all be investigated with the present methodology.

The general nature of problems that can be analyzed with the TRUMP program should make it a useful tool for inverse heat transfer applications. For gun barrel applications, where it is very difficult to measure bore surface temperatures, it is desirable to use measured temperature histories to backout the surface temperatures or heat flux into the solid. Methods such as given by Beck (5) and Lavrentiev, et al (6) could be used with TRUMP to analyze barrel temperature data such as given by Elbe (7).

REFERENCES

1. A. L. Edwards, "TRUMP: A Computer Program for Transient and Steady State Temperature Distributions in Multidimensional Systems," LRL Livermore, UCRL-14754 (1972) Rev. 3.
2. A. L. Edwards, "A Compilation of Thermal Property Data for Computer Heat Conduction Calculations," LRL Livermore, UCRL-50589 (1969).
3. H. S. Carslaw and J. C. Jaeger, Conduction of Heat in Solids, Oxford University Press, 1959.
4. D. Schauer, "FED: A Computer Program to Generate Geometric Input for the Heat Transfer Code TRUMP," UCRL-50816, 1973.
5. J. V. Beck, "Non-Linear Estimation Applied to the Nonlinear Inverse Heat Conduction Problem," *Int. J. Heat and Mass Transfer*, v. 13, pp. 703-716, 1970.
6. M. M. Lavrentiev, et al., "Multidimensional Inverse Problems for Differential Equations," (Lecture Notes in Mathematics, v. 167), Springer Verlag, 1970.
7. R. E. Elbe, "External Barrel Temperature of the M16A1 Rifle," ADA019649 (R-TR-75-045), Rock Island Arsenal, 1975.

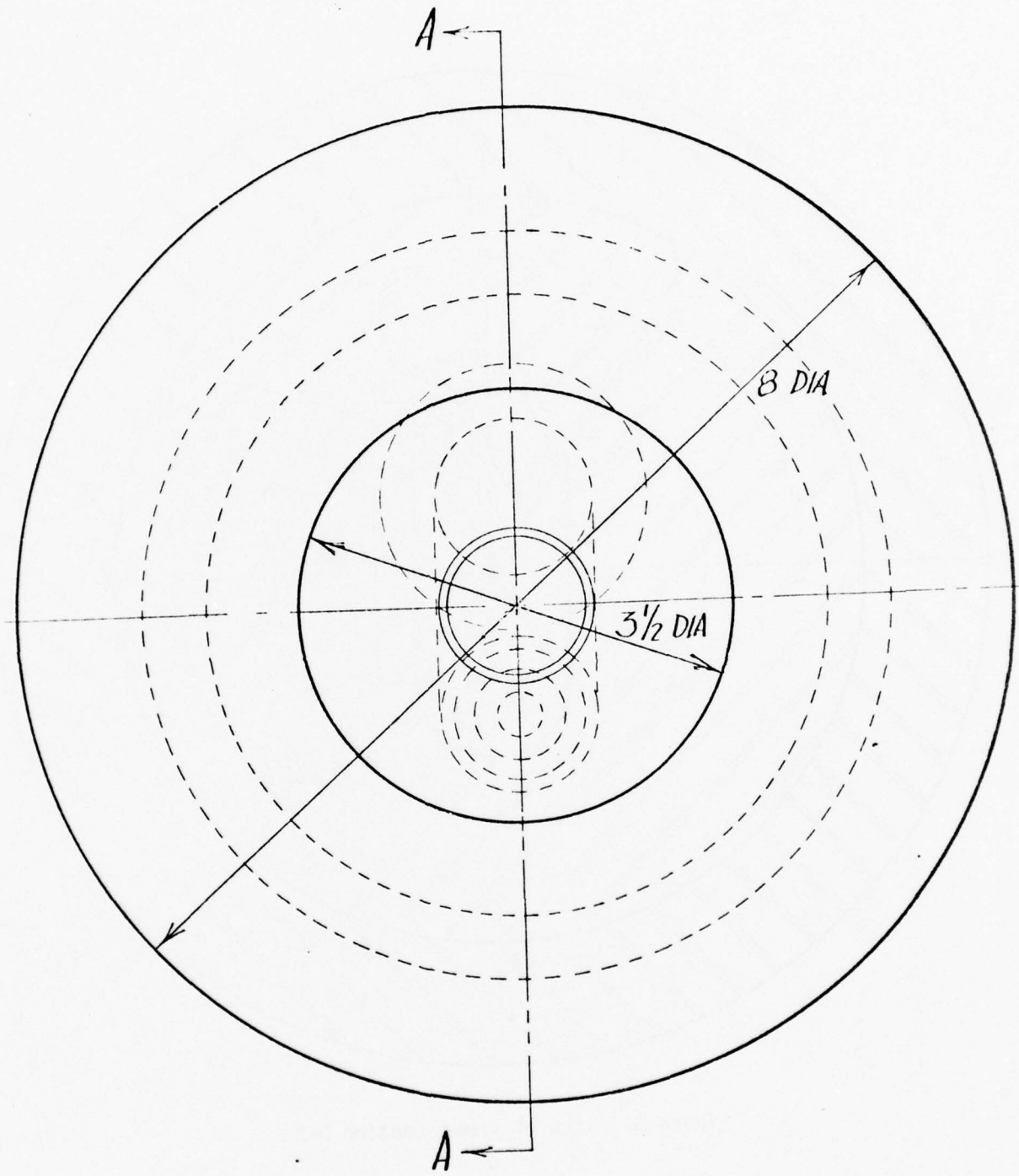


Figure 2. End View of the Breech Region

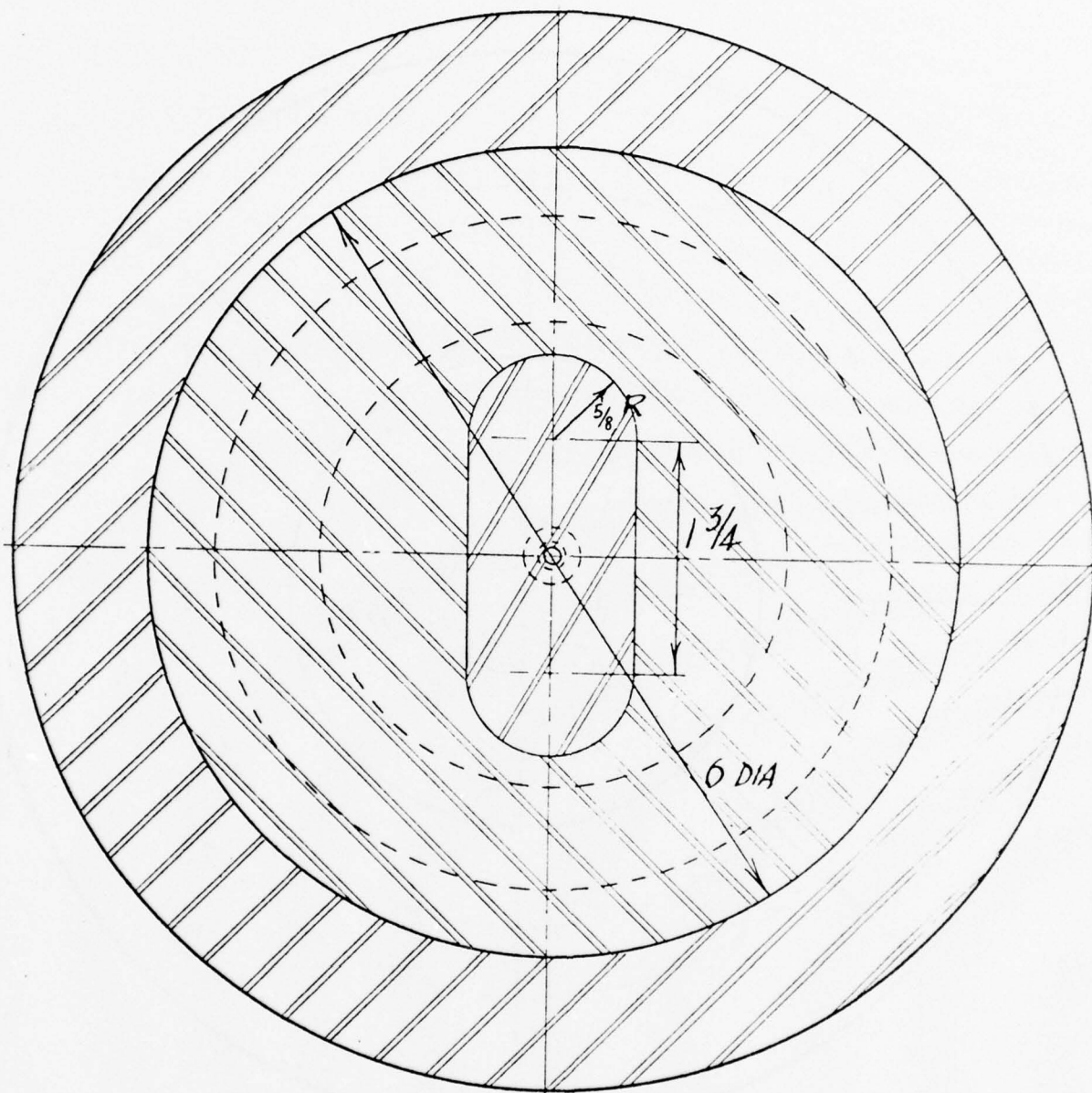


Figure 3. View of Cross Section B-B

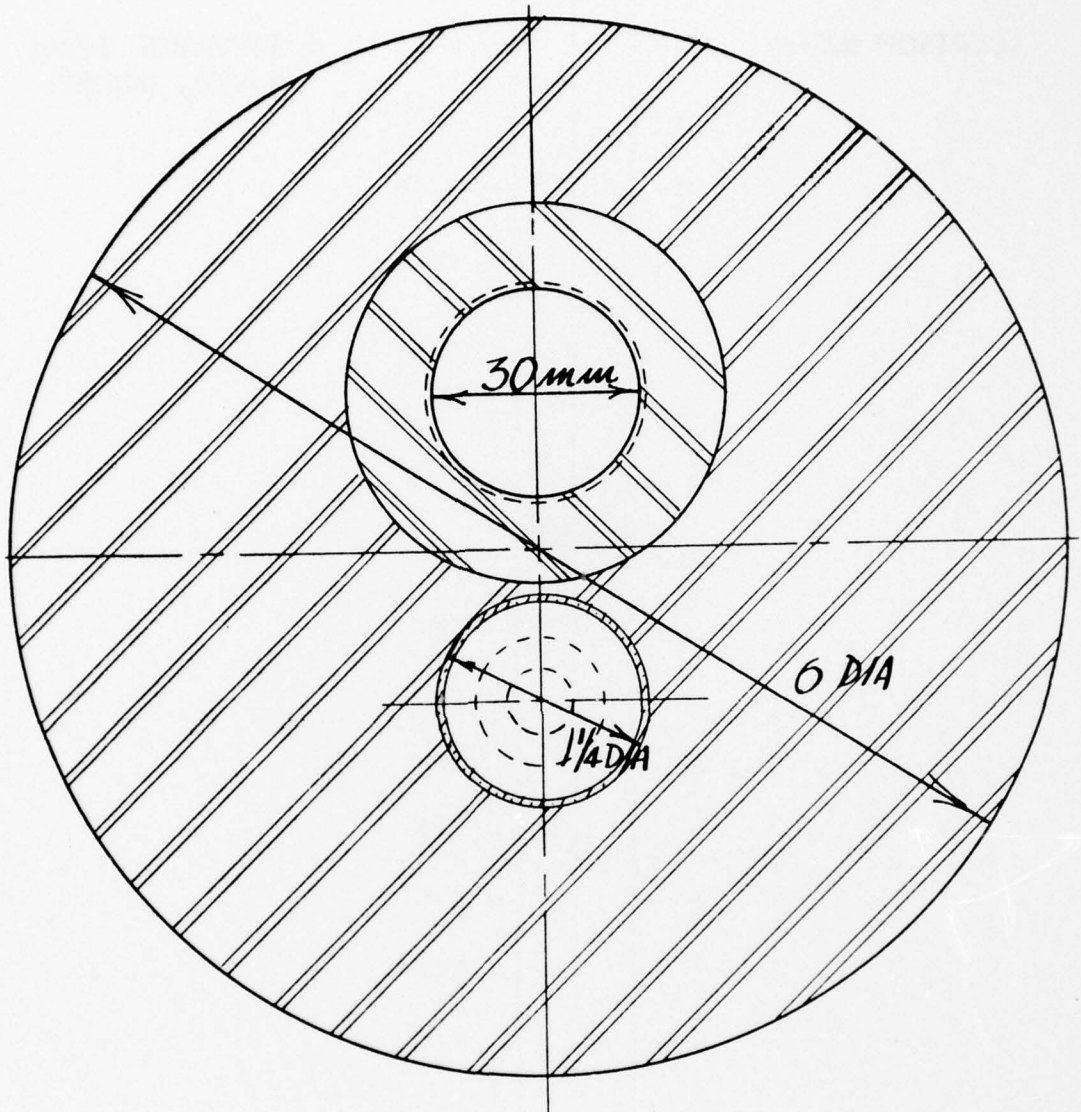


Figure 4. View of Cross Section C-C

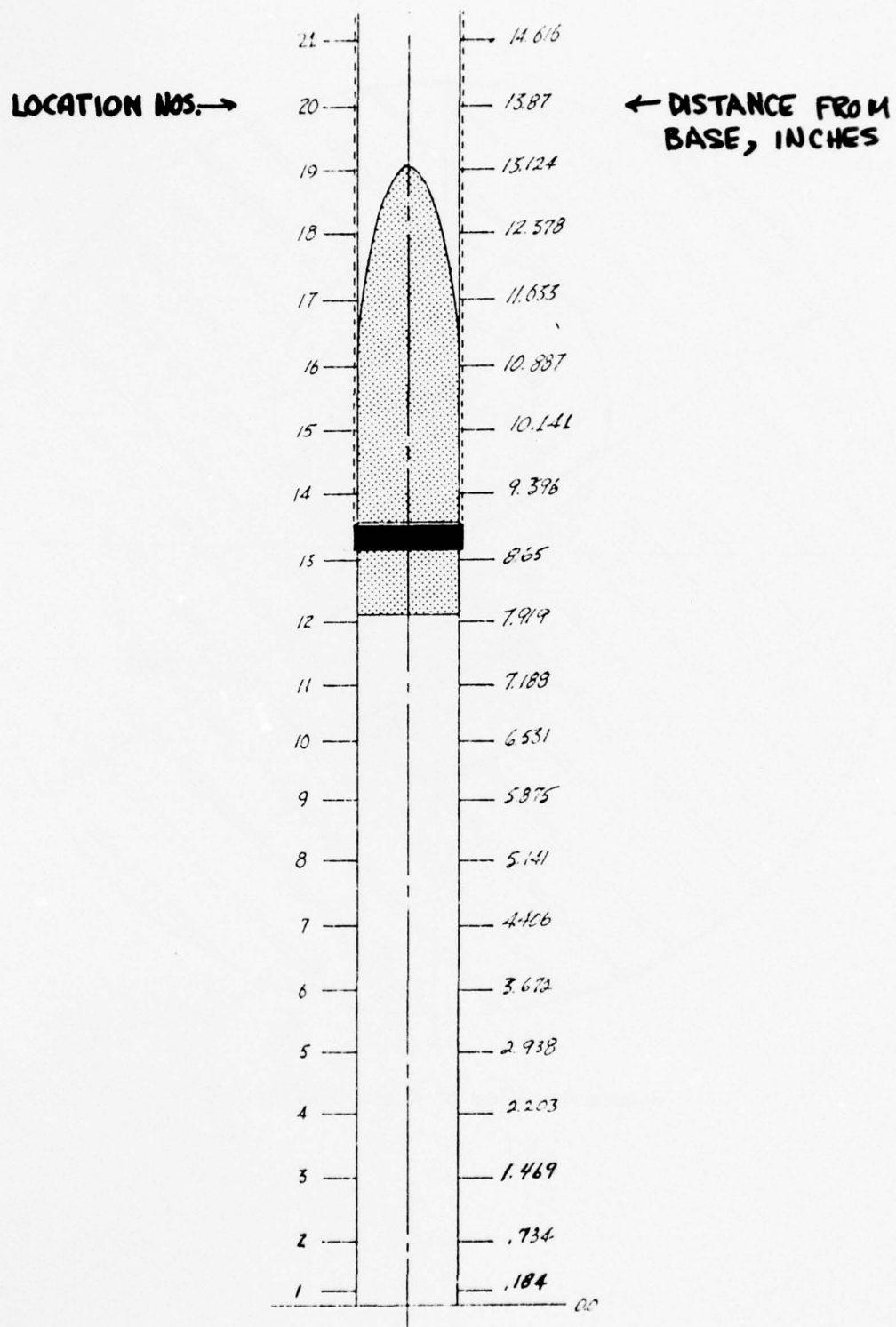


Figure 5. Cross Section of the Geometry for Which the Boundary Conditions were Generated

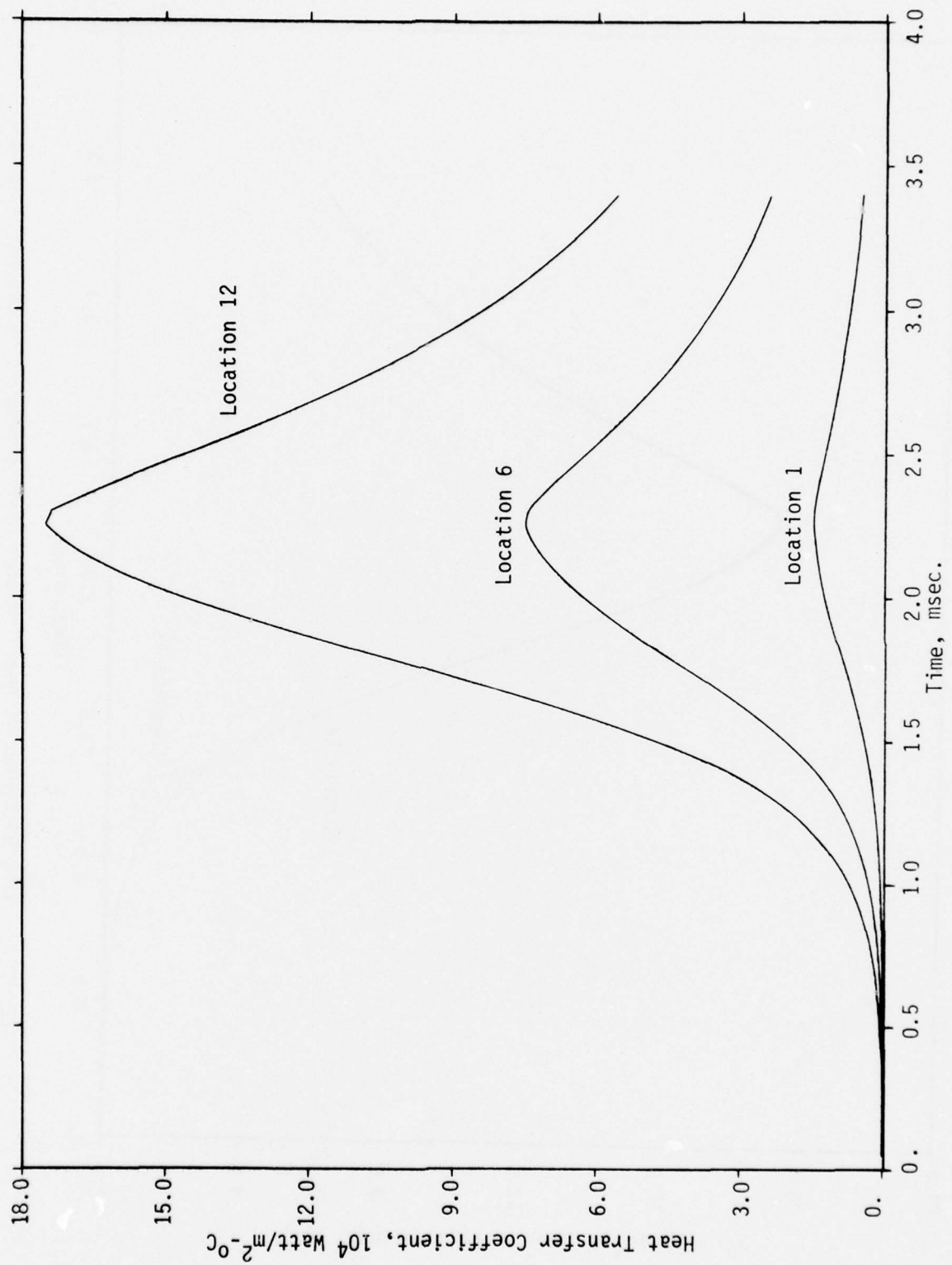


Figure 6. Time Histories of Heat Transfer Coefficients at Locations 1, 6, and 12

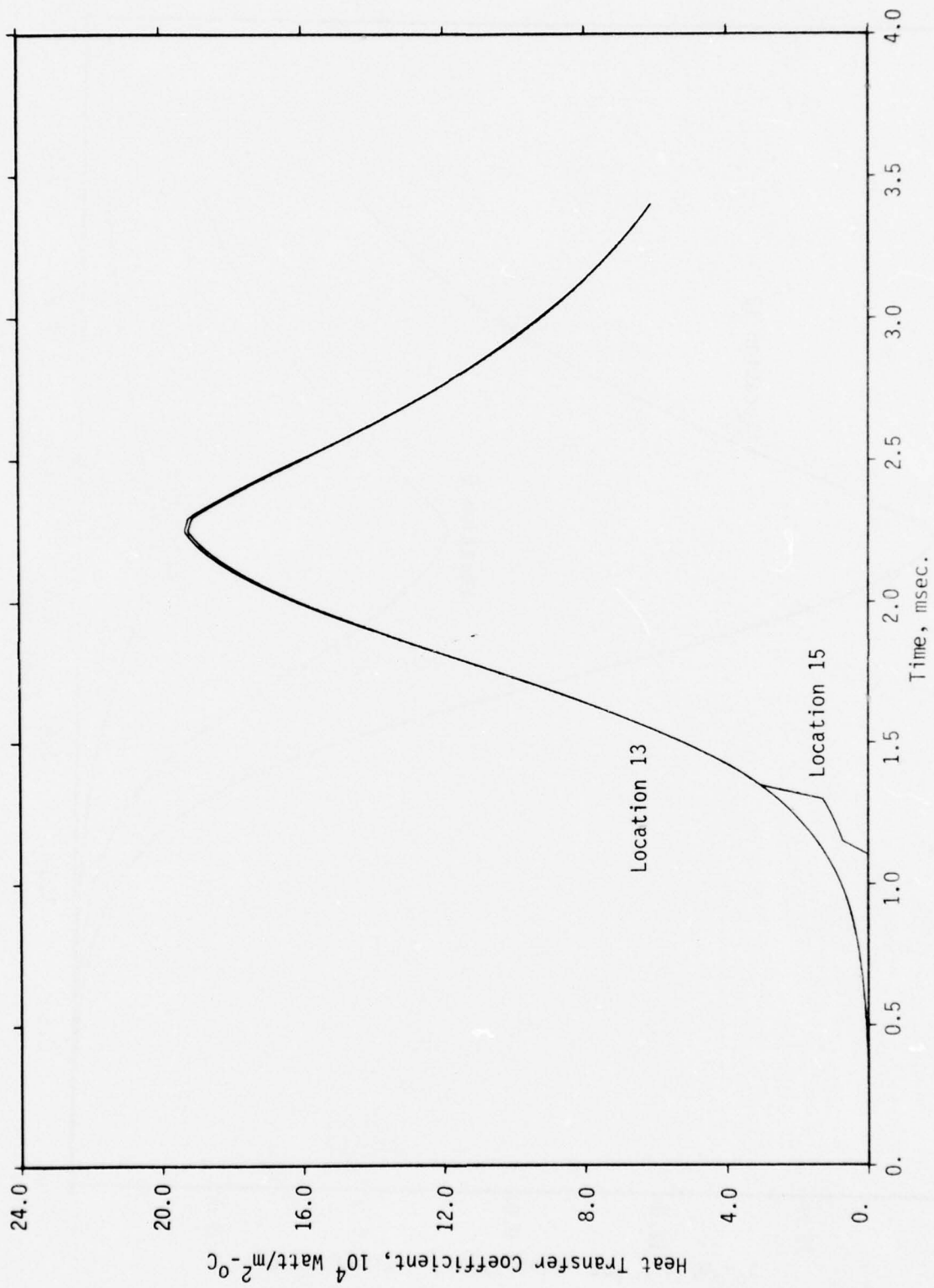


Figure 7. Time Histories of Heat Transfer Coefficients at Locations 13 and 15

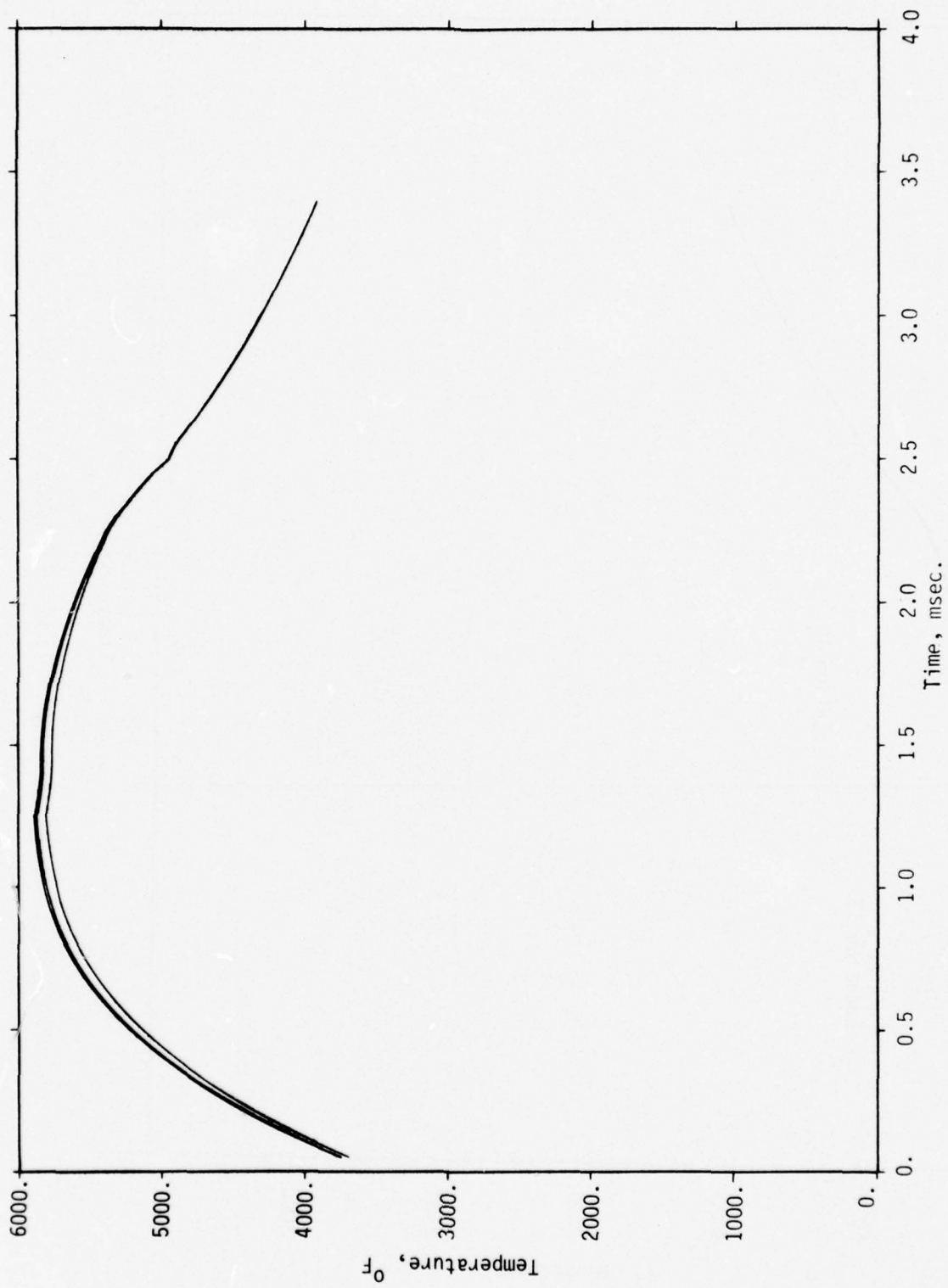


Figure 8. Time Histories of Bulk Fluid Temperatures at Locations 1, 6 and 12

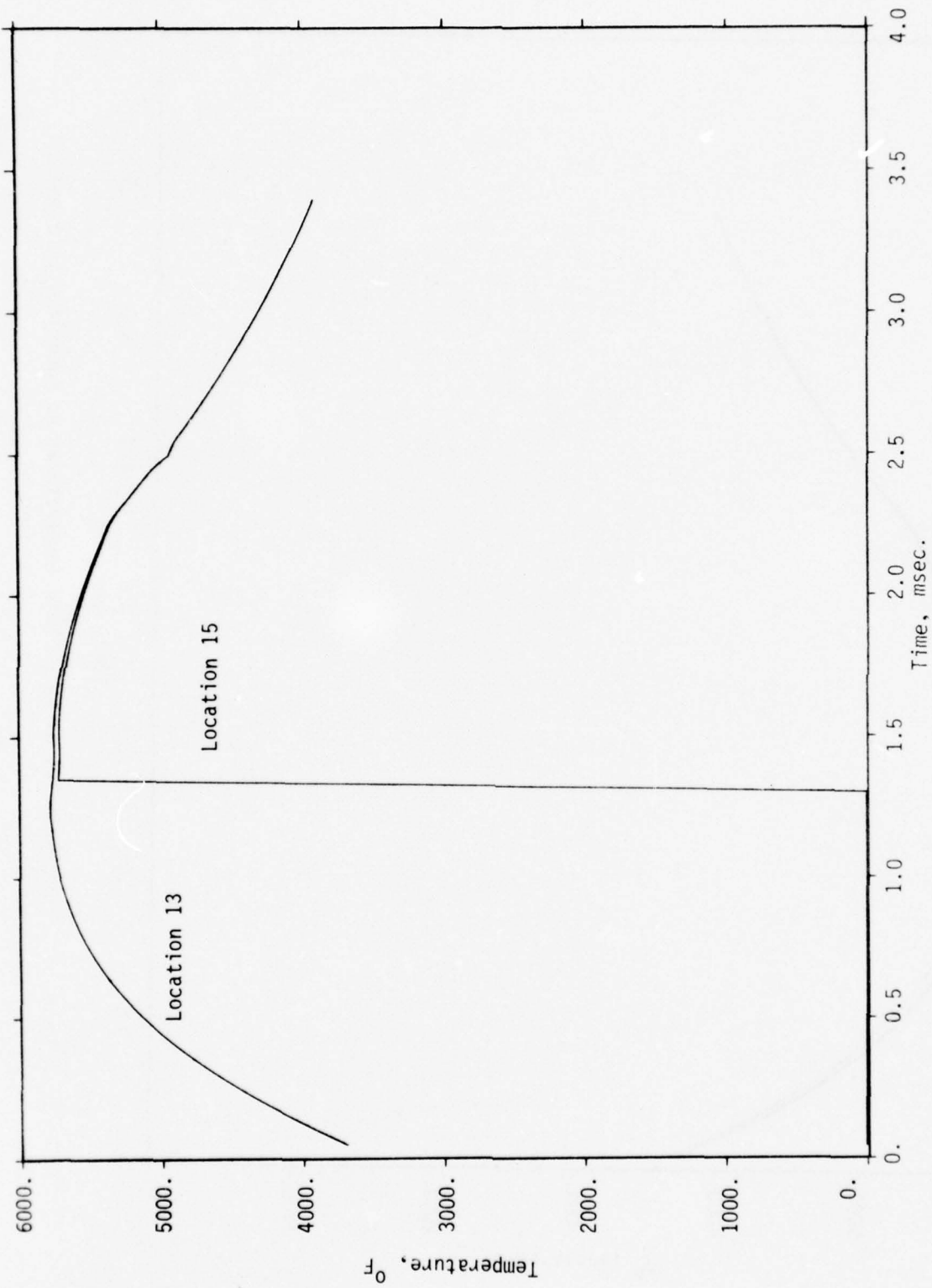


Figure 9. Time Histories of Bulk Fluid Temperatures at Locations 13 and 15

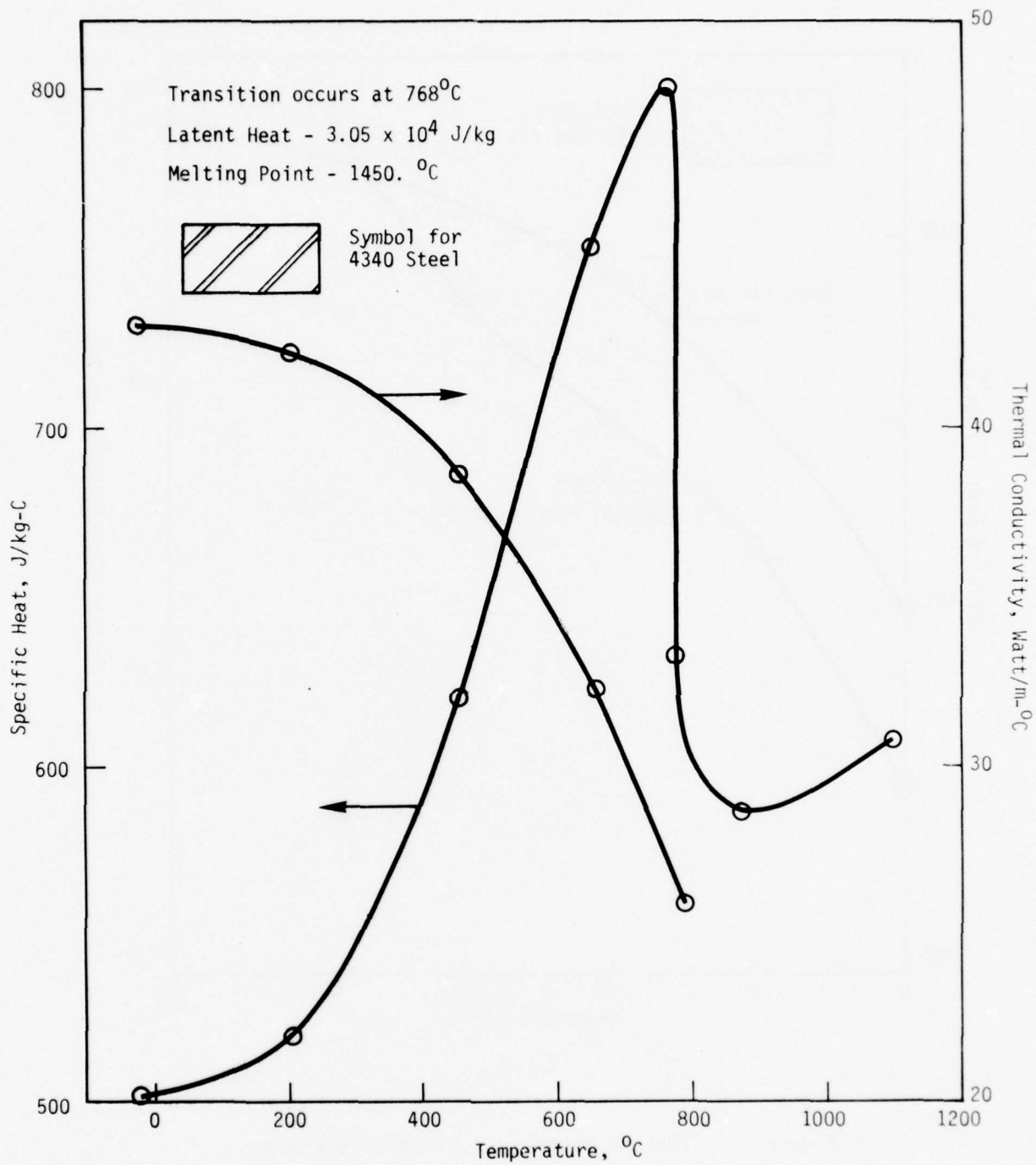


Figure 10. Thermal Properties of SAE 4340 Steel

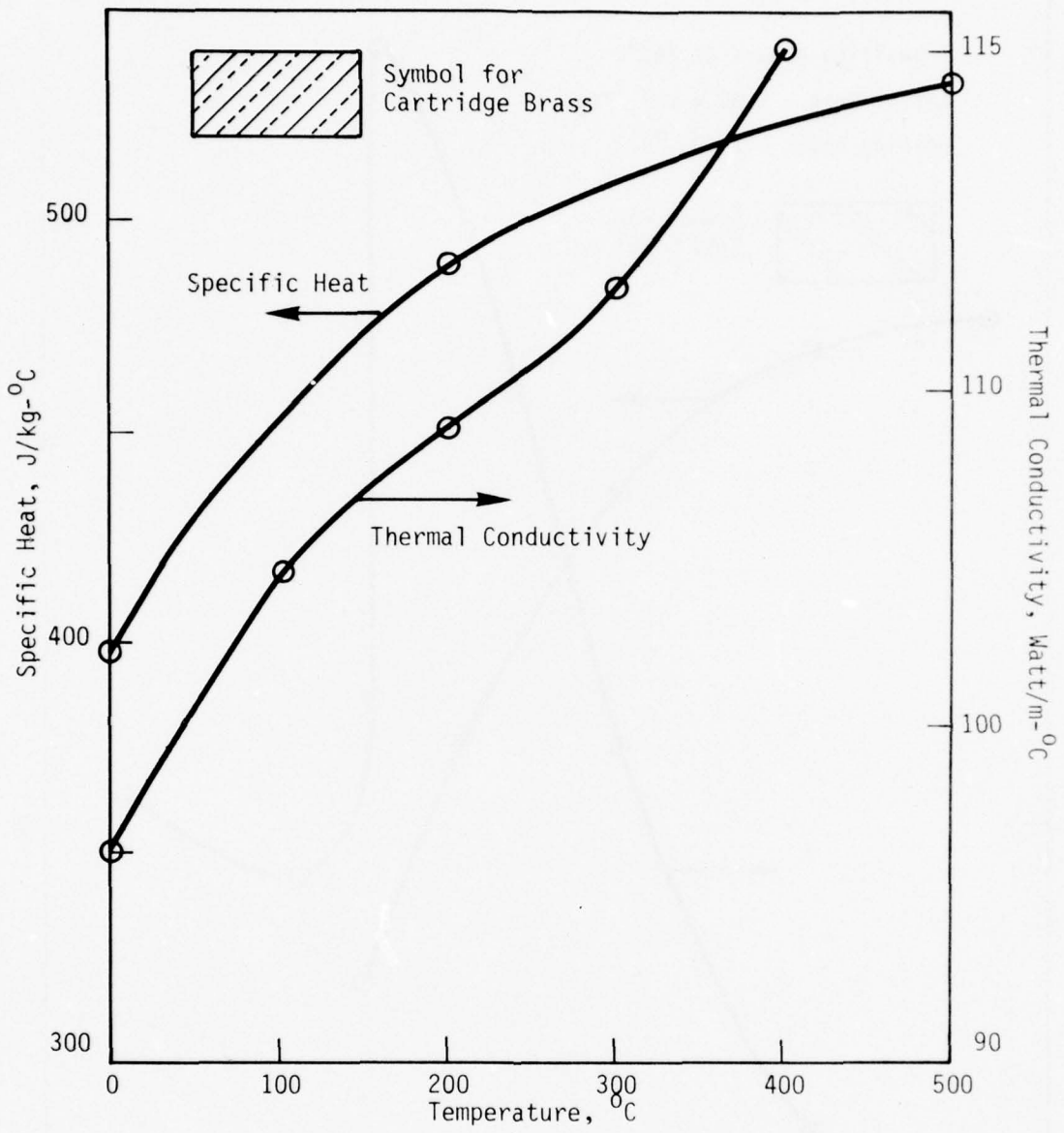


Figure 11. Thermal Properties of Cartridge Brass

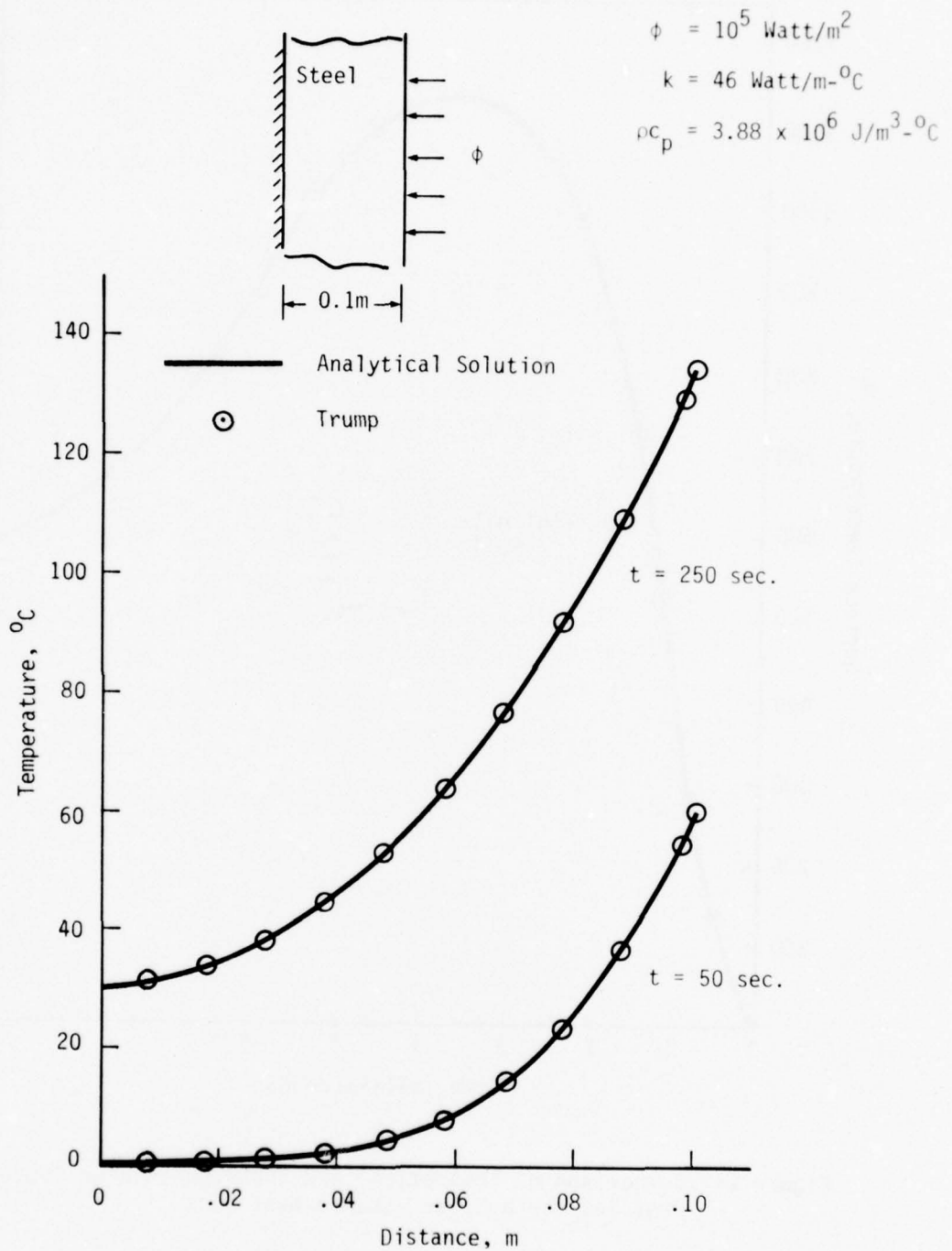


Figure 12. Comparison of Theoretical and TRUMP Calculated Temperature Profiles for a Rectangular Slab with a Constant Heat Flux on One Face and Insulated at the Other

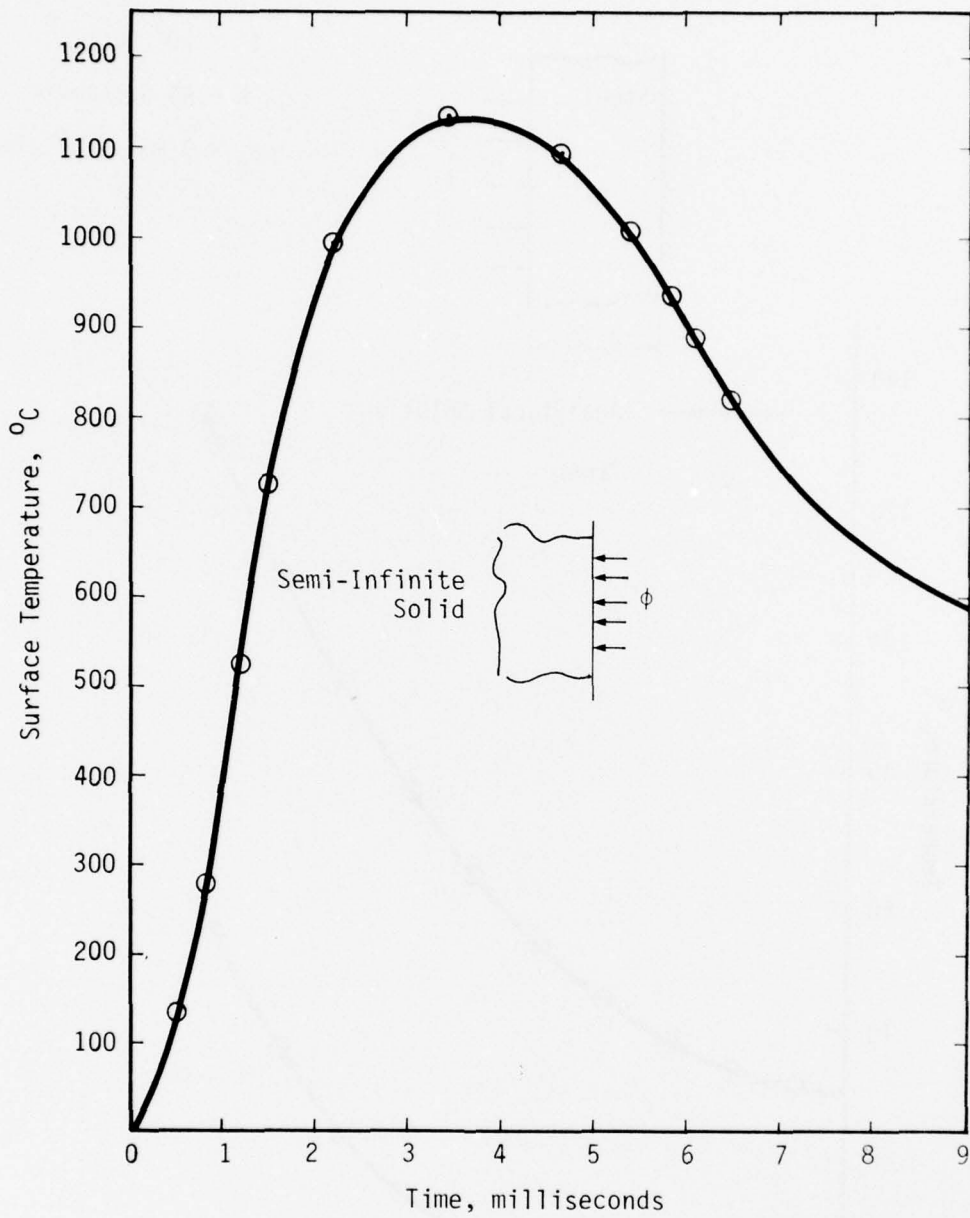


Figure 14. Comparison of Theoretical and TRUMP Calculated Temperature Profiles for a Spike Shaped Heat Flux

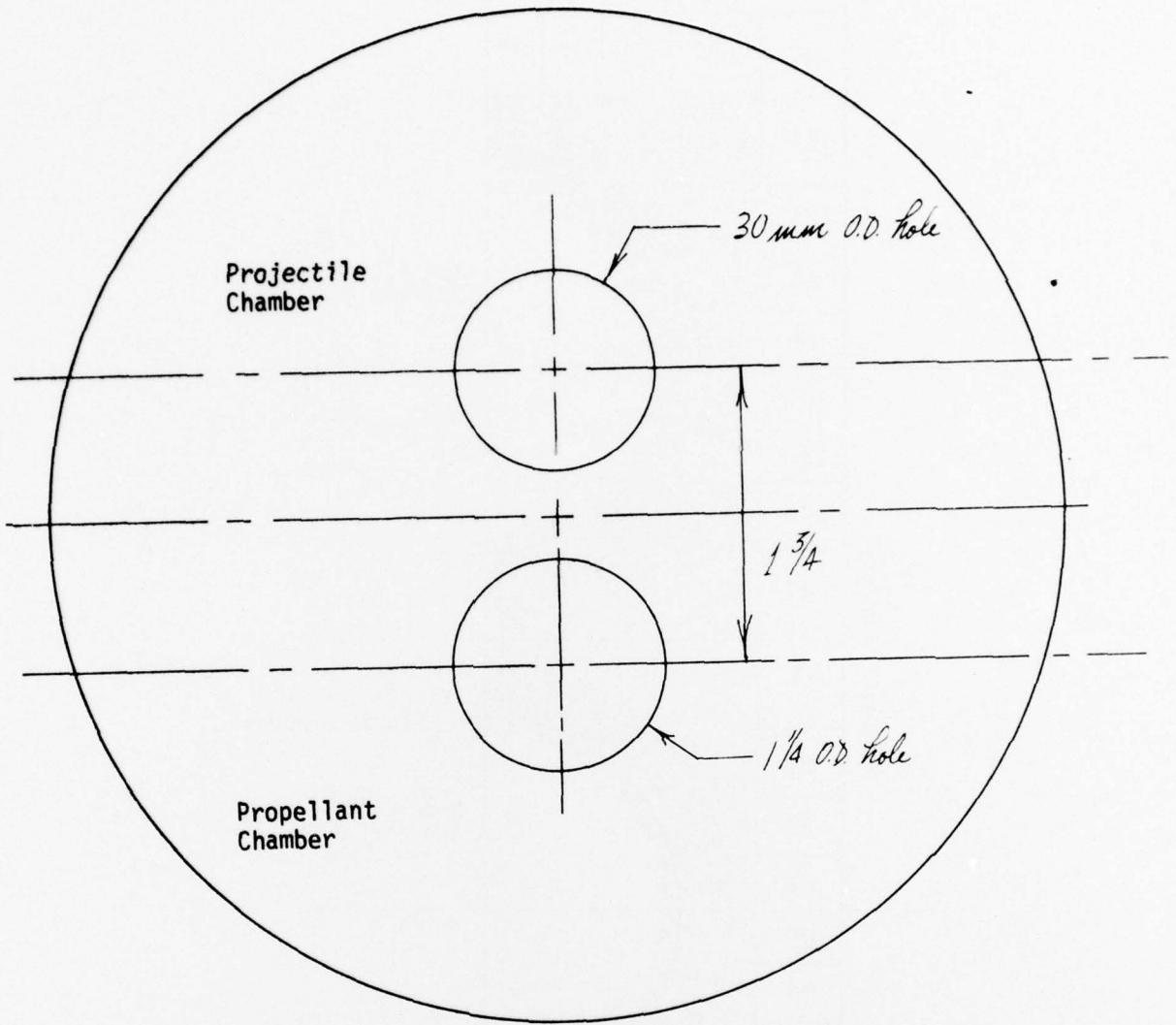


Figure 15. Representative Cross Section of the Gun Tube Chamber

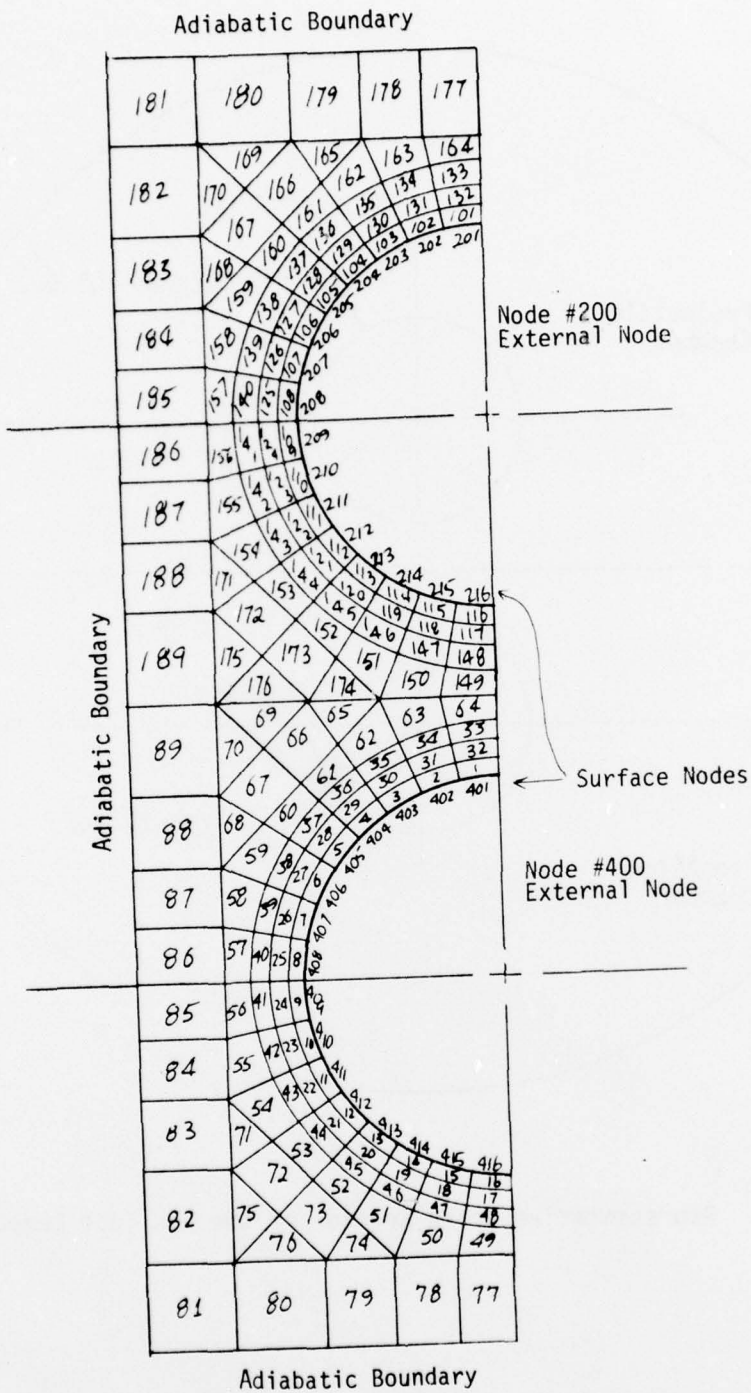


Figure 16. Node Configuration No. 3

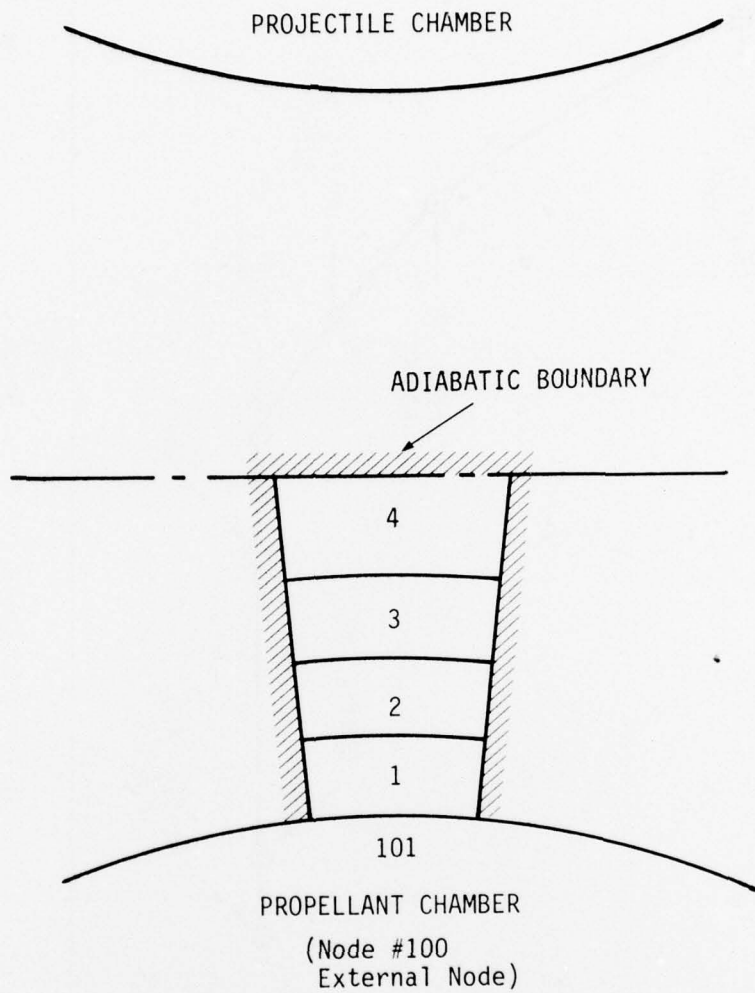


Figure 17. NODE CONFIGURATION #5

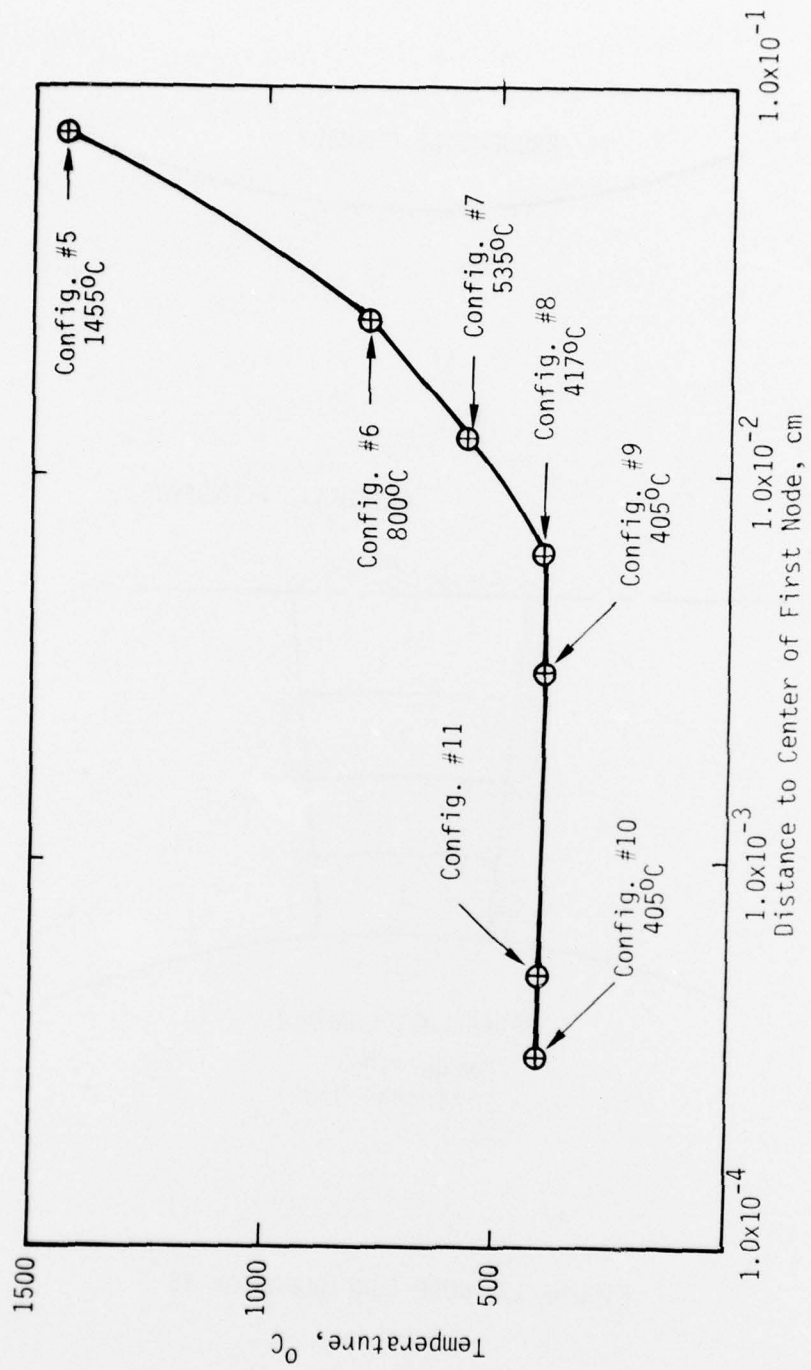


Figure 18. Dependency of the Computed Surface Temperature on the Node Size

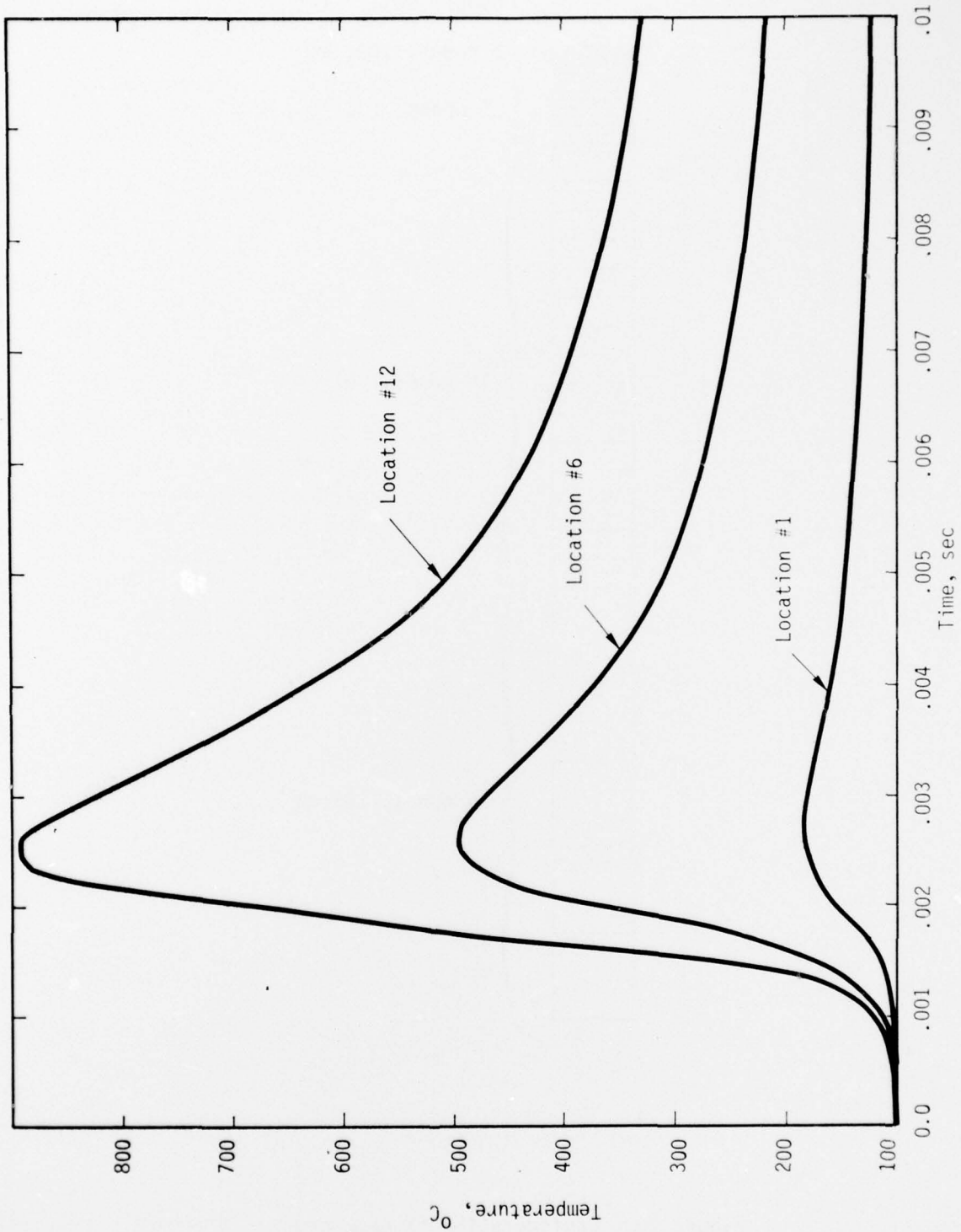


Figure 19. Surface Temperature History at Three Locations on the Gun Tube Using Configuration No. 10.

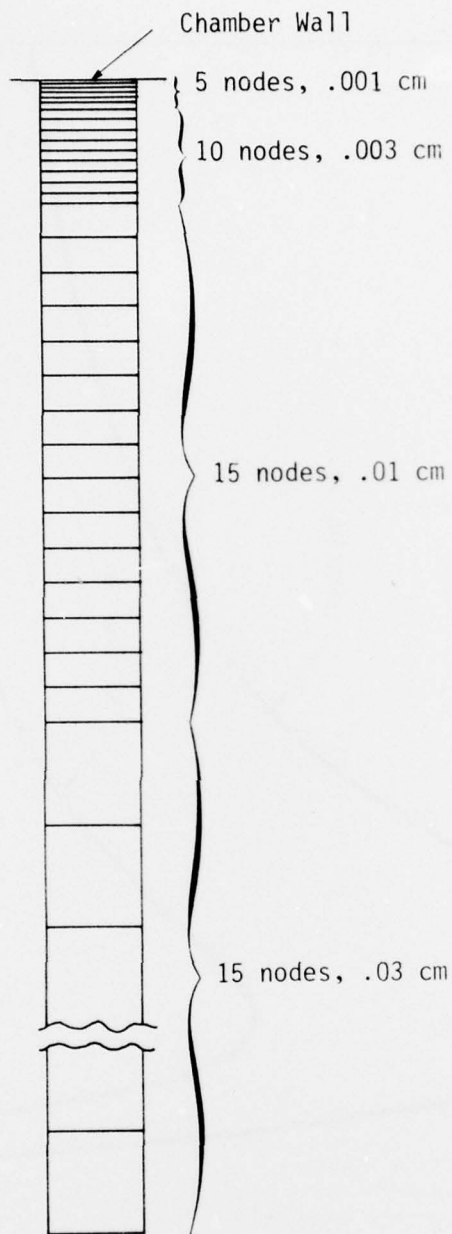


Figure 20. Configuration 11 Geometry

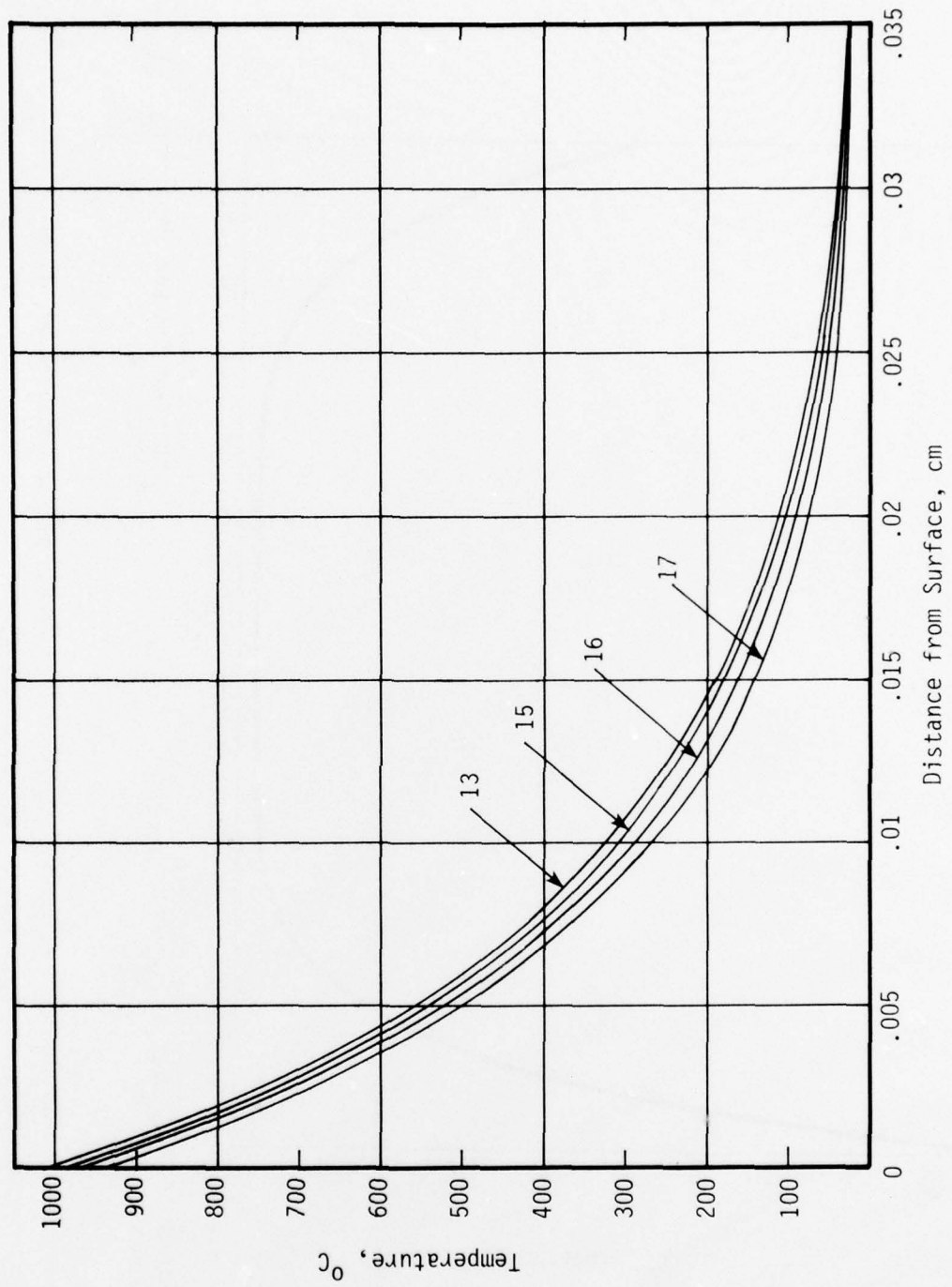


Figure 21. Spatial Temperature Distributions at the Time of Peak Surface Temperature at Locations 13, 15, 16, and 17.

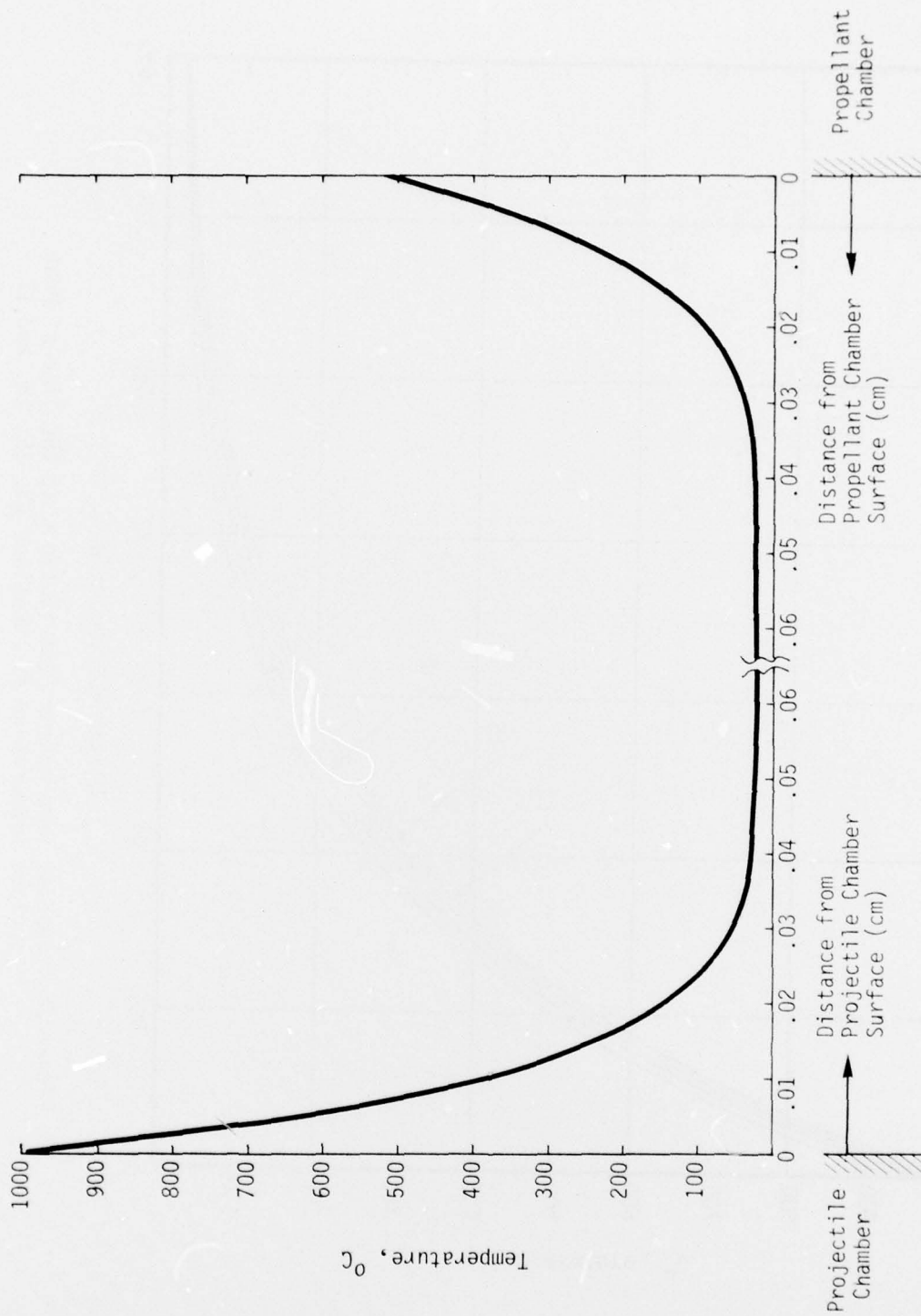


Figure 22. Temperature Distribution Across Web at Location No. 13 at Time of Peak Surface Temperature.

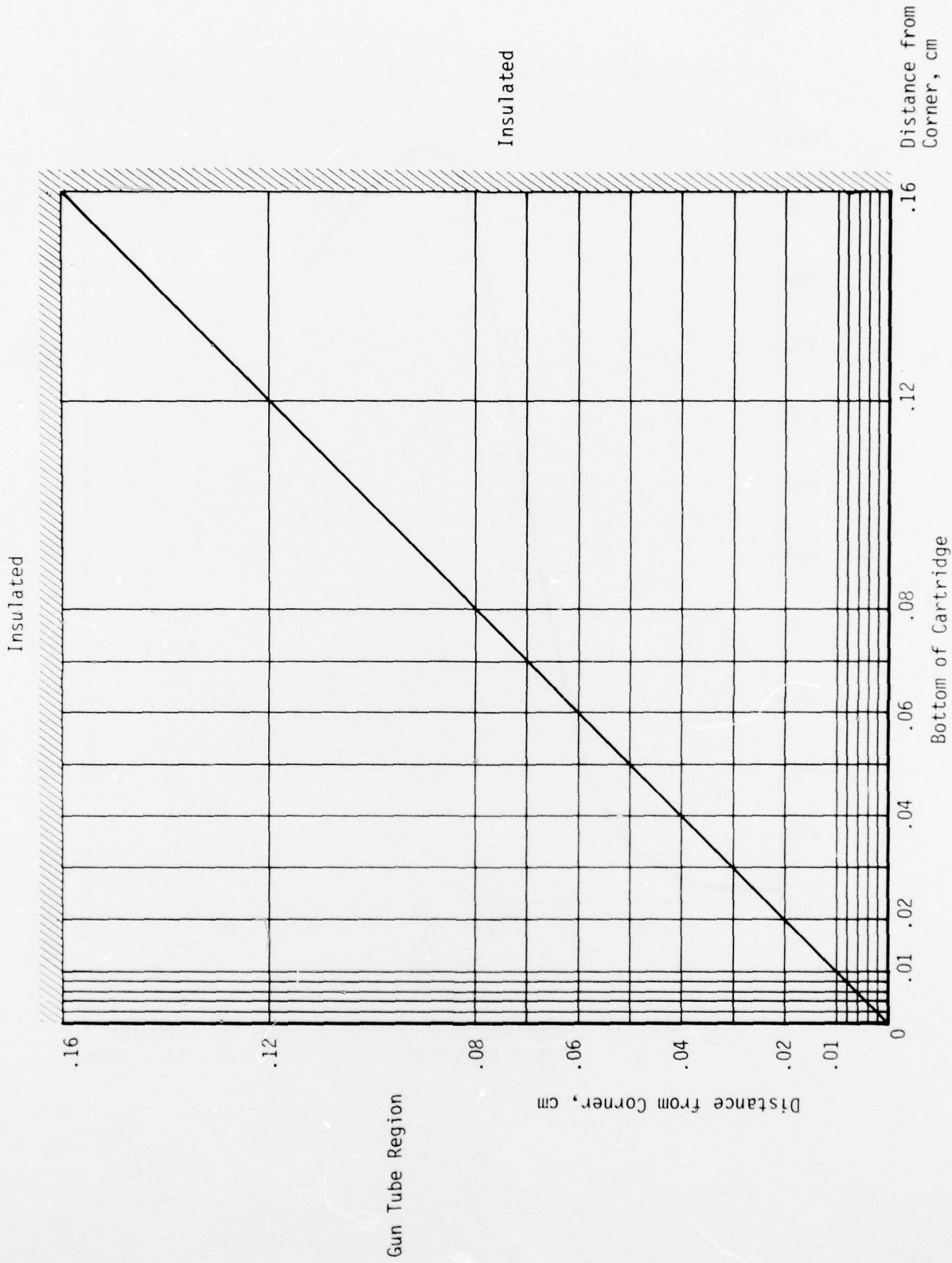


Figure 23. Interior Corner Region Node Geometry

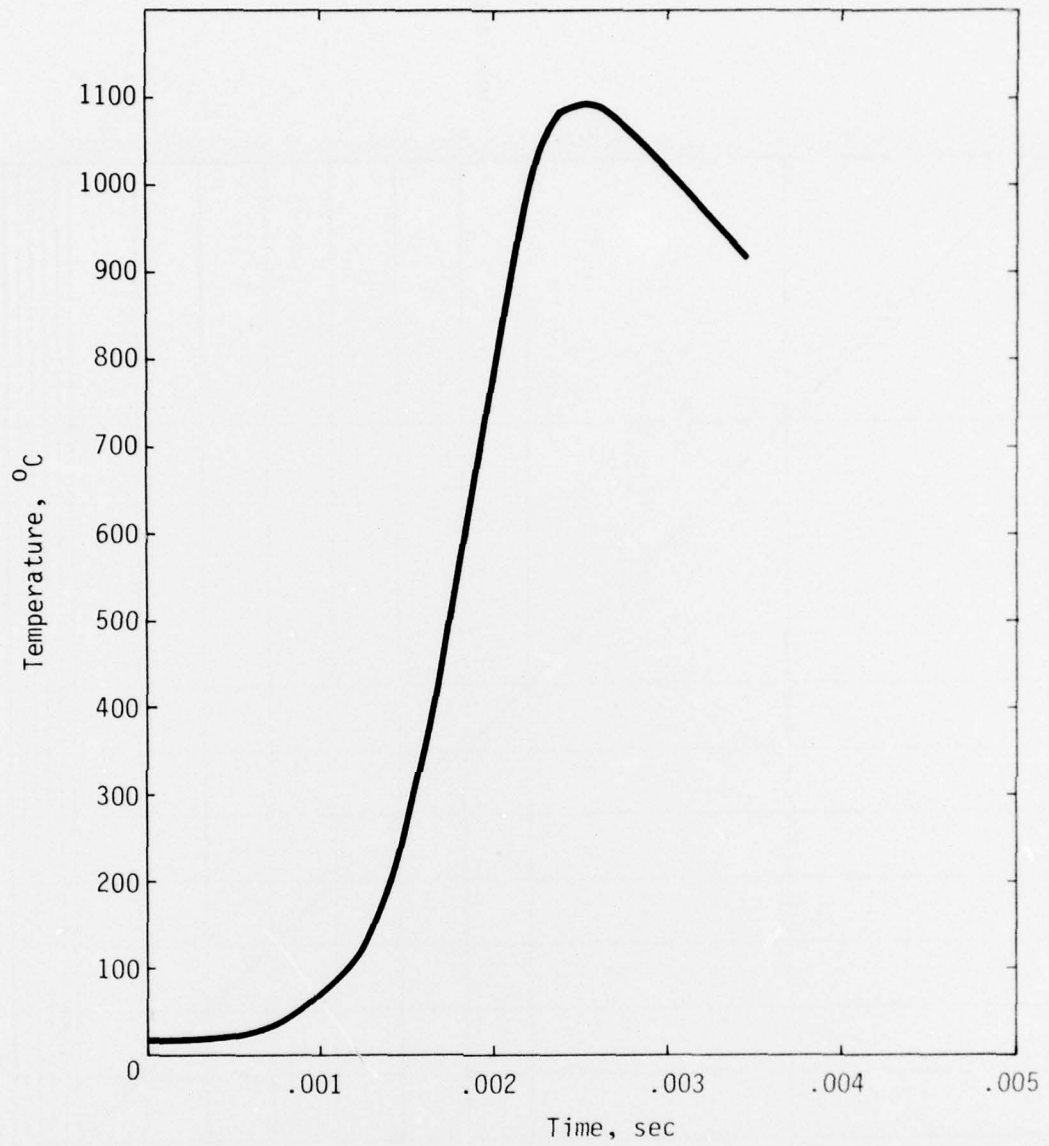


Figure 24. Temperature-time History for the Interior Corner Region Peak Temperature Surface Node.

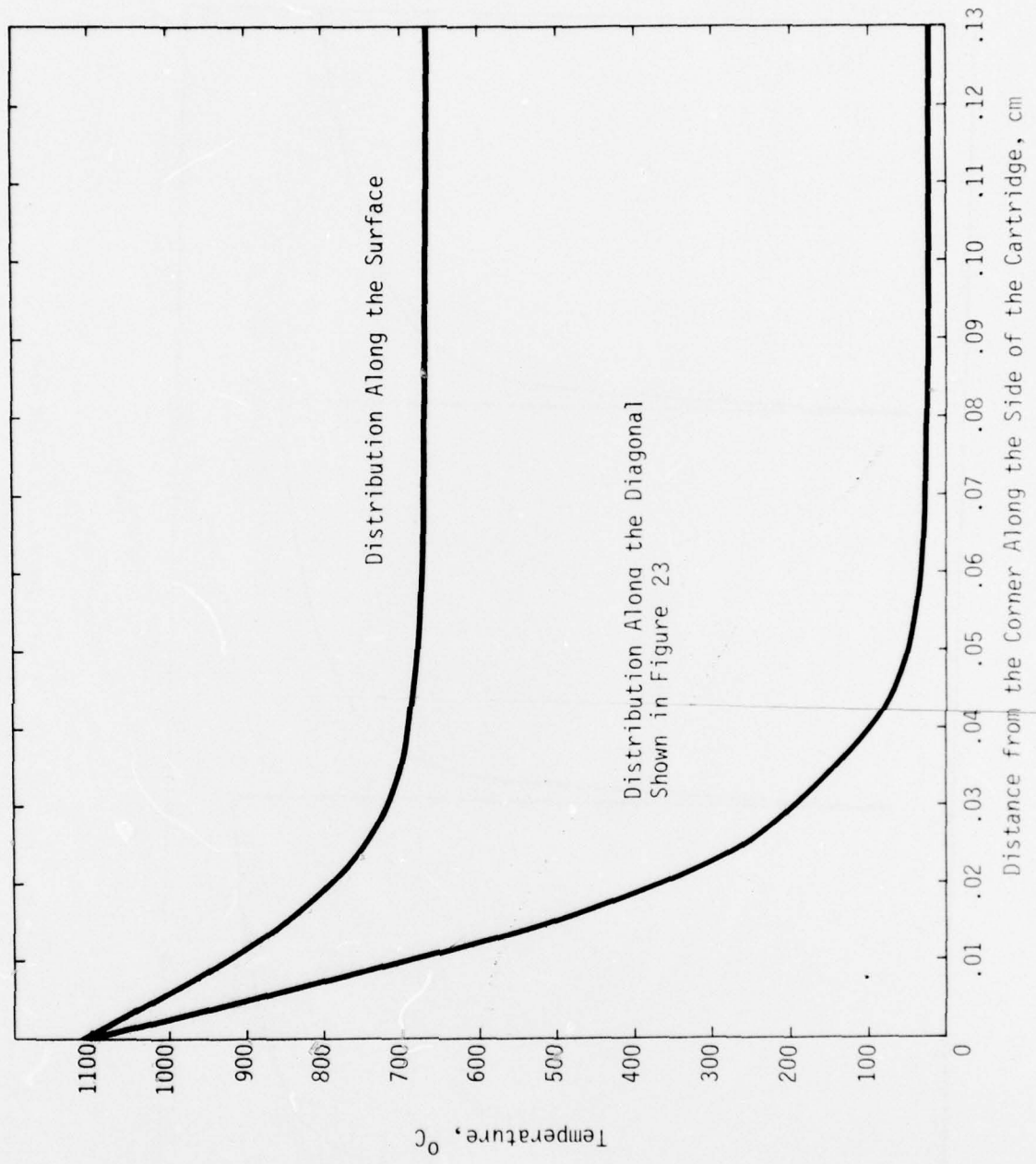


Figure 25. Spatial Temperature Profiles for the Interior Corner Regions.

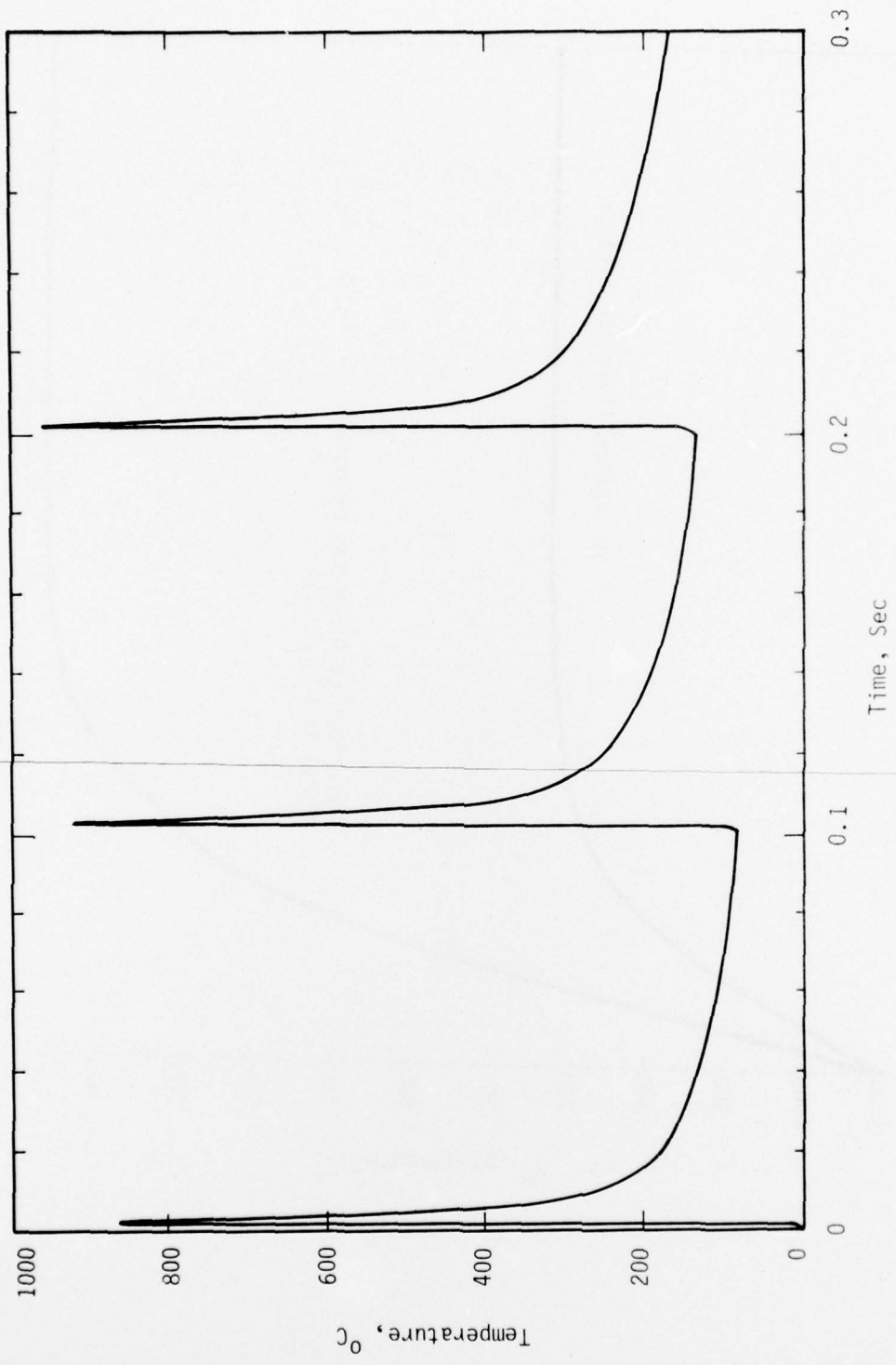


Figure 26. TEMPERATURE HISTORY AT LOCATION #12 FOR MULTIPLE (3) FIRINGS

DISTRIBUTION LIST

<u>No. of Copies</u>	<u>Organization</u>	<u>No. of Copies</u>	<u>Organization</u>
12	Commander Defense Documentation Center ATTN: DDC-TCA Cameron Station Alexandria, VA 22314	2	Commander US Army Mobility Equipment Research & Development Command ATTN: Tech Docu Cen, Bldg. 315 DRSME-RZT Fort Belvoir, VA 22060
1	Commander US Army Materiel Development and Readiness Command ATTN: DRCDMA-ST 5001 Eisenhower Avenue Alexandria, VA 22333	1	Commander US Army Armament Research and Development Command ATTN: DRDAR-TD Dover, NJ 07801
1	Commander US Army Aviation Systems Command ATTN: DRSVA-E 12th and Spruce Streets St. Louis, MO 63166	1	Commander US Army Armament Research and Development Command ATTN: DRDAR-FCV, Stan Goodman Philadelphia, PA 19137
1	Director US Army Air Mobility Research and Development Laboratory Ames Research Center Moffett Field, CA 94035	1	Commander US Army Harry Diamond Labs ATTN: DRXDO-TI 2800 Powder Mill Road Adelphi, MD 20783
1	Commander US Army Electronics Research and Development Command ATTN: DRDEL-RD Fort Monmouth, NJ 07703	1	Director US Army TRADOC Systems Analysis Activity ATTN: ATAA-SA White Sands Missile Range, NM 88002
2	Commander US Army Missile Research and Development Command ATTN: DRDMI-R Redstone Arsenal, AL 35809	1	Commander US Army Research Office ATTN: CRD-AA-IP P.O. Box 12211 Research Triangle Park NC 27709
1	Commander US Army Tank-Automotive Development Command ATTN: DRDTA-RWL Warren, MI 48090	1	Director Lawrence Livermore Laboratory ATTN: Tech Info Div P.O. Box 808 Livermore, CA 94550

DISTRIBUTION LIST

<u>No. of Copies</u>	<u>Organization</u>
1	Director Los Alamos Scientific Lab ATTN: Rept Lib P.O. Box 1663 Los Alamos, NM 87544
1	Mathematical Applications Group, Inc. ATTN: E. Troubetzkoy 3 Westchester Plaza Elmsford, NY 10523
1	Science Applications, Inc. ATTN: P.L. Versteegen 8400 Westpark Drive McLean, VA 22101

Aberdeen Proving Ground

Marine Corps Ln Ofc
Dir, USAMSAA